

Performance Evaluation and Diversity Analysis of RIS-Assisted Communications Over Generalized Fading Channels in the Presence of Phase Noise

IMÈNE TRIGUI¹ (Member, IEEE), WESSAM AJIB¹ (Senior Member, IEEE),
WEI-PING ZHU² (Senior Member, IEEE), AND MARCO DI RENZO³ (Fellow, IEEE)

¹Département d'informatique, Université du Québec à Montréal, Montréal, QC H2L 2C4, Canada

²Department of Electrical and Computer Engineering, Concordia University, Montreal, QC H3G 1M8, Canada

³Laboratoire des Signaux et Systèmes, CNRS, CentraleSupélec, Université Paris-Saclay, 91192 Gif-sur-Yvette, France

CORRESPONDING AUTHOR: I. TRIGUI (e-mail: trigui.imene@uqam.ca)

The work of Marco Di Renzo was supported in part by the European Commission through the H2020 ARIADNE Project under Grant 871464 and through the H2020 RISE-6G Project under Grant 101017011.

ABSTRACT In this paper, we develop a unified theoretical framework for analyzing the outage performance of reconfigurable intelligent surfaces (RISs)-assisted communication systems over generalized fading channels and in the presence of phase noise. Fox's H function theory is then utilized to derive the outage probability for various channel fading and phase noise distributions in closed-form. We further conduct an asymptotic outage analysis to obtain insightful findings. In particular, we present the maximum diversity order achievable over such channels and demonstrate the performance variation in comparison to conventional Rayleigh channels. Then, based on upper bounds and lower bounds, we propose a design criteria for RISs to achieve the maximum diversity order in the presence of phase noise. More specifically, we show that if the absolute difference between pairs of phase errors is less than $\pi/2$, RIS-assisted communications achieve the full diversity order over independent fading channels, even in the presence of phase noise. The theoretical frameworks and findings are validated with the aid of Monte Carlo simulations.

INDEX TERMS Reconfigurable intelligent surface, Fox's H-distribution, rice fading, phase noise, outage probability, diversity order.

I. INTRODUCTION

CONTEMPORARY wireless networks modeling and analysis are vibrant topics that keep taking new dimensions in complexity, as researchers explore the potential of innovative breakthrough technologies to support the upcoming Internet of Things (IoT) and 6G era [1]. Among these emerging technologies, reconfigurable intelligent surfaces (RISs) [2]–[6] have been introduced with an overarching vision of artificially controlling the wireless environment for increasing the quality of service and spectrum efficiency. RIS technology is based on the massive integration of low-cost tunable passive elements on large surfaces, which can be deployed on, e.g., the facades of buildings, and are

able to, e.g., reflect and modulate the incident RF signals, which leads to a more controllable wireless environment [5] and a more efficient implementation of multi-antenna transmitters [7]. Leveraging these key properties, RIS-enabled networks challenge device-side approaches, such as massive multiple-input-multiple-output (MIMO) systems, encoding, modulation, and relaying, which are currently deployed in wireless networks in order to fully adapt to the time-variant and unpredictable channel states [4], [5]. Due to the potential opportunities offered by RIS-empowered wireless networks, a large body of research contributions have recently appeared in the literature. The interested readers are referred to the survey papers in [2]–[6], where a comprehensive description of

TABLE 1. Performance analysis frameworks and diversity analysis available in the literature (N = number of reconfigurable elements of the RIS).

Ref.	Channel Model	Phase Noise	Method of Analysis	Diversity Order (without phase noise)	Diversity Order (with phase noise)
[15]	Rayleigh	No	Laguerre Series	$\frac{N}{2} \frac{\pi^2}{16-\pi^2}$ (as for the CLT)	-
[16]	Rayleigh	No	Gamma Approximation	N	-
[17]	Rayleigh	No	Method in [36]	N	-
[18]	Arbitrary	Yes	Large N , Nakagami Distr.	m in [18, Eq. (12)]	m in [18, Eq. (12)]
[19]	Rayleigh	L -bit Quant.	Bounds	N	$< \frac{N+1}{2}$ if $L = 2$; N if $L \geq 3$
[20]	Rayleigh	Yes	Large N , Gamma Approx.	$1/AF$ in [20, Eq. (20)]	$1/AF$ in [20, Eq. (20)]
[21]	Rayleigh	No	\mathcal{GK} Approximation	N	-
[23]	Rayleigh	No	Chernoff Bound	N	-
[24]	Rayleigh	1-bit Quant.	Gamma Approximation	N	$(N + 1)/2$
[25]	Rice	No	Method in [36]	N	-
[26]	Rayleigh	No	\mathcal{GK} Approximation	N	-
[34]	Nakagami- m	No	CLT and Gil Pelaez [35]	-	-
This	Arbitrary Fox's H	Arbitrary	Exact and Bounds	see (13)	see Prop. 9

\mathcal{GK} stands for Generalized \mathcal{K} distribution [48, Table IIV].

the state-of-the-art, the scientific challenges, the distinctive differences with other technologies, and the open research issues are discussed.

A. RELATED WORKS

Several research papers have appeared recently, mostly considering application scenarios where the line-of-sight link is either too weak or is not available, and, therefore, an RIS is employed to enable the reliable transmission of data through the optimization of the phase shifts of its individual reconfigurable elements [7], and of the precoding and decoding vectors at the transmitter and receiver, respectively, e.g., [8], [9]. Specifically, both [7] and [8] demonstrate the necessity of jointly optimizing the transmit beamforming and phase shifts for a well designed RIS. In this regard, several RIS-aided designs have been recently proposed for various advanced communication techniques, including millimeter-wave communications [10], unmanned aerial vehicle networks [11], physical layer security [12], and simultaneous wireless information and power transfer [13]. However, there exist limited research efforts that have explored the communication-theoretic performance limits of RIS-aided communications [14]–[26], and, therefore, a limited number of results are available to date. A major research issue for analyzing the fundamental performance limits of RIS-aided systems is the analysis of the exact distribution of the RIS end-to-end equivalent channel. To circumvent this open issue, some recent attempts for studying RIS-aided systems include the use of approximate distributions and asymptotic analysis [14]–[26]. Under the assumption of Rayleigh fading, it was shown in [14], [16], [17] that the distribution of a single RIS equivalent channel follows a modified Bessel function. In [18] and [19], an RIS-aided transmission system in the presence of phase errors was considered, and the composite channel was shown to be equivalent to a point-to-point Nakagami- m fading channel by using the central limit theorem (CLT). However, it is known that the CLT is inaccurate when the number of reconfigurable elements of the RIS is small. Recent results, in addition, showed that the approximation error attributed

to the CLT can be significant in the high signal-to-noise-ratio (SNR) regime [14]. Approximations for the received SNR in the presence of multiple randomly deployed RISs were introduced in [27], and an asymptotic analysis of the data rate and channel hardening effect in an RIS-aided large antenna-array system was presented in [28]. As far as the fading channel is concerned, the Rayleigh fading model has been commonly assumed, with only some exceptions that incorporated the line-of-sight (LoS) channel, yet only under the scope of phase optimization, e.g., [29], [30]. However, Rayleigh fading may have limited legitimacy in RIS-aided communications in which the RIS is appropriately deployed to leverage the LoS paths for enhancing the received power [31]. Recently, the authors of [32]–[34] considered the Nakagami- m fading channels by leveraging CLT-based or moment-based Gamma approximations.

In Table 1, we summarize the communication-theoretic frameworks that, to the best of our knowledge, are available in the literature. We evince that analytical studies have been conducted predominantly over Rayleigh fading channels and that no exact analytical framework exists. In addition, the analysis of the diversity order of RIS-assisted communication systems is still an open issue. There is, however, general consensus that the CLT is not a suitable tool for analyzing the diversity order, since it yields accurate approximations in the low-SNR regime [14]. In this paper, we propose new analytical methods for overcoming these limitations.

B. CONTRIBUTIONS

As a step forward to fill the mentioned research gaps, this work leverages fundamental results from Fox's H-transform theory for analyzing the performance of RIS-aided wireless communications. More precisely, we introduce a new analytical framework that provides exact analytical expressions of the outage probability for several widely used generalized fading models in the absence of phase noise. The proposed method for performance evaluation is endowed with high flexibility to capture a broad range of fading distributions, thereby unveiling the diversity order of RIS-aided networks and generalizing the results available for transmission over

Rayleigh fading. In addition, we introduce a new approach for analyzing the diversity order of RIS-aided systems over generalized fading channels in the presence of phase noise. The proposed approach confirms the unsuitability of the CLT for analyzing the diversity order of RIS-aided systems, and unveils the achievable diversity order under general fading channels and phase noise distributions. With the aid of lower bounds and upper bounds, more precisely, we identify sufficient conditions for achieving the full diversity order in RIS-assisted systems. The main contributions of this paper can be summarized as follows.

- We propose a new analytical framework for analyzing the performance of RIS-aided systems, which leverages Fox's H transform theory for modeling, in a unified fashion, general RIS-induced fading environments in terms of outage probability and achievable diversity. This paper, to the best of our knowledge, is the first to unify the outage analysis over many fading without resorting to any restrictive assumption or approximation.
- We draw multiple link-level design insights from the proposed analysis. For instance, we show that the diversity order in the absence of phase noise scales with the number of reconfigurable elements of the RIS multiplied by a factor that depends of the worst fading distribution of the transmitter-RIS and RIS-receiver links.
- We study the transmission through an RIS whose phase shifts deviate from the ideal values according to general phase noise distributions, and discuss how the presence of errors in the phase shifts influences the achievable diversity. We demonstrate, in particular, that a sufficient condition for achieving the full diversity order is that the absolute difference between pairs of phase errors is less than $\pi/2$.

The rest of this paper is organized as follows. Section II describes the system model and the considered fading distributions. Sections III and IV are devoted to the unified performance analysis framework, where the outage probability and the diversity order of RIS-assisted communications are analyzed in the presence of perfect and imperfect phase shifts, respectively. Simulation and numerical results are discussed in Section V. Finally, Section VI concludes the paper.

II. SYSTEM MODEL

We consider an RIS with N reconfigurable elements, which are arranged in a uniform array of tiny antennas spaced half of the wavelength apart and whose phase response is locally optimized, assuming full channel state information (CSI) knowledge at the RIS.¹ We assume that the RIS transmits data to a single antenna receiver by reflecting an incident RF wave emitted by a single antenna transmitter. More specifically, we assume that the direct transmission link between the transmitter and the receiver is blocked, and, thus, the

1. The generalization of this work to consider imperfect and statistical CSI at the RIS is a promising direction for future research.

RIS is deployed to relay the scattered signal and to leverage virtual LoS paths for enhancing the strength of the received signal. The received SNR of the considered system is [3]

$$\gamma = \rho \left| \sum_{i=1}^N h_i g_i e^{j\phi_i} \right|^2, \quad (1)$$

where ρ is the average SNR of the RIS-assisted link, h_i and g_i , $i = 1, 2, \dots, N$ are independent² complex coefficients that characterize the channels between the transmitter and the RIS, and the RIS and the receiver, respectively, and ϕ_1, \dots, ϕ_N are the phase shifts that are optimized to maximize the SNR at the receiver.³ In particular, ρ in (1) includes the path-loss of the end-to-end RIS channel, as described in, e.g., [37]–[39], which is assumed to be fixed and given in this paper. The impact of channel estimation errors and overhead is not explicitly discussed in the present paper, but it can be taken into account as recently described in [41].

Assumption 1: The amplitudes $|h_i|$ and $|g_i|$ are independent and non-identically distributed (i.n.i.d) Fox's H-distributed random variables (RVs) whose probability density function (pdf) is

$$f_{|y_i|}(x) = \kappa_i^y H_{p_i^y, q_i^y}^{m_i^y, n_i^y} \left[c_i^y x \left| \begin{matrix} (a_{ij}, A_{ij})_{j=1:p_i^y}^y \\ (b_{ij}, B_{ij})_{j=1:q_i^y}^y \end{matrix} \right. \right], \quad (2)$$

where $y \in \{h, g\}$, and $H[\cdot]$ stands for the Fox's H function [43, eq. (1.2)]. The Fox H distribution subsumes a large number of conventional and generalized fading distributions widely used in wireless communications, such as Rayleigh, Nakagami-m, and Weibull fading.

Usually, the RISs are positioned to exploit the LoS path with respect to the location of the transmitter to increase the received power. In this case, Rician fading is a better small-scale fading model in the presence of a LoS path. However, the Rician distribution does not belong to the family of distributions in (2). Therefore, we consider a further generalized fading model.

Assumption 2: Using the hyper-Fox's H-distribution [42], the pdf of a Rician fading channel is

$$f_{|y_i|}(x) = \sum_{k=0}^{\infty} \kappa_k^y H_{0,1}^{1,0} \left[c_k^y z \left| \begin{matrix} - \\ (k + \frac{1}{2}, \frac{1}{2}) \end{matrix} \right. \right], \quad (3)$$

where $c_k^y = \sqrt{K^y + 1}$, $\kappa_k^y = \frac{e^{-K^y} \sqrt{K^y + 1}}{k! \Gamma(k+1)}$, and K^y for $y \in \{h, g\}$ denotes the Rice factors of the transmitter-RIS and RIS-receiver links, respectively.

In the following sections, by leveraging the H-transform, we establish a unified framework for analyzing the

2. The assumption of independent channel coefficients is made for analytical tractability and is justified, as a first-order approximation, if the reconfigurable elements of the RIS are spaced half of the wavelength apart. The generalization of the proposed analytical framework in the presence of channel correlation is postponed to future research works.

3. The amplitude of each reflection coefficient is set to unity, which represents an ideal scenario. The generalization of this work to phase-dependent amplitude variation [40] is a promising direction for future research.

performance of RIS-assisted communications where the fading envelope is described by the Fox's H-distribution for non-specular small-scale fading and the hyper Fox's H-distribution under LoS propagation. Perfect and imperfect phase shifts are analyzed.

III. OUTAGE PROBABILITY - NO PHASE NOISE

The optimal design for the phase shifts of an RIS-assisted link consists of setting the phase shift of each element ϕ_i so that all phase contributions due to the phase of h_i , i.e., $\angle h_i$ and the phase of g_i , $\angle g_i$, $i = 1, \dots, N$, are compensated [3]. Accordingly, substituting $\phi_n = -\angle(h_n + g_n)$, $n = 1, \dots, N$, in (1), the outage probability in the absence of phase noise is $P(\rho(\sum_{i=1}^N |h_i||g_i|)^2 < \gamma_{th}) = P(\sum_{i=1}^N |h_i||g_i| < \sqrt{\rho_t})$, where $\rho_t = \gamma_{th}/\rho$. An analytical expression of the outage probability is given in the following proposition.

Proposition 1: The outage probability with optimal phase shifts is

$$\Pi(\rho, N) = \tau \mathbf{H}_{0,1:\tilde{p}_1, \tilde{q}_1, \dots, \tilde{p}_N, \tilde{q}_N}^{0,0:\tilde{m}_1, \tilde{n}_1, \dots, \tilde{m}_N, \tilde{n}_N} \left[\begin{array}{c} \tilde{c}_1 \sqrt{\rho_t} \\ \vdots \\ \tilde{c}_N \sqrt{\rho_t} \end{array} \middle| \begin{array}{l} -(1, 1), (\delta_1, \Delta_1) \tilde{p}_1; \dots; (1, 1), (\delta_N, \Delta_N) \tilde{p}_N \\ (0; 1, \dots, 1): (\xi_1, \Xi_1) \tilde{q}_1; \dots; (\xi_N, \Xi_N) \tilde{q}_N \end{array} \right], \quad (4)$$

where $\tau = \prod_{i=1}^N \frac{\kappa_i^h \kappa_i^g}{c_i^h c_i^g}$, $\tilde{c}_i = c_i^h c_i^g$, with

$$(\delta_i, \Delta_i) \tilde{p}_i = \left((a_{ij} + A_{ij}, A_{ij})_{j=1:p_i^h}^h, (a_{ij} + A_{ij}, A_{ij})_{j=1:p_i^g}^g \right), \quad (5)$$

$$(\xi_i, \Xi_i) \tilde{q}_i = \left((b_{ij} + B_{ij}, B_{ij})_{j=1:q_i^h}^h, (b_{ij} + B_{ij}, B_{ij})_{j=1:q_i^g}^g \right), \quad (6)$$

and $\tilde{m}_i = m_i^h + m_i^g$, $\tilde{n}_i = n_i^h + n_i^g + 1$, $\tilde{q}_i = q_i^h + q_i^g$, $\tilde{p}_i = p_i^h + p_i^g + 1$, and $H[\dots, \cdot]$ is the multivariable Fox's H-function whose definition in terms of Mellin-Barnes contour integrals is given according to [43, Definition A.1] as

in (7), shown at the bottom of this page, where $\Gamma(\cdot)$ is the gamma function [52].

Proof: See Appendix A. ■

Proposition 2: The outage probability of RIS-assisted communications in Rice fading is

$$\Pi(\rho, N) = \sum_{k_1, \dots, k_N=0}^{\infty} \sum_{t_1, \dots, t_N=0}^{\infty} \tau \mathbf{H}_{0,1:1,2, \dots, 1,2}^{0,0:2,1, \dots, 2,1} \left[\begin{array}{c} \Delta \sqrt{\rho_t} \\ \vdots \\ \Delta \sqrt{\rho_t} \end{array} \middle| \begin{array}{l} -(1, 1); \dots; (1, 1) \\ (0; 1, \dots, 1): (k_1 + 1, \frac{1}{2}), (t_1 + 1, \frac{1}{2}); \dots; (k_N + 1, \frac{1}{2}), (t_N + 1, \frac{1}{2}) \end{array} \right], \quad (8)$$

where $\Delta = \sqrt{(1 + K^h)(1 + K^g)}$ and $\tau = \prod_{i=1}^N \frac{e^{-K^h} K^{h k_i}}{k_i! \Gamma(k_i + 1)} \frac{e^{-K^g} K^{g t_i}}{t_i! \Gamma(t_i + 1)}$.

Proof: We use the distribution in (3) and apply the same procedure as for the proof of (4).

Moreover, if M terms are used in (8), we can define the truncation error as

$$\mathcal{E}(M) = \sum_{k_1, \dots, k_N=M+1}^{\infty} \sum_{t_1, \dots, t_N=M+1}^{\infty} \tau \Theta(\infty), \quad (9)$$

where

$$\Theta(y) = \mathbf{H}_{0,1:1,2, \dots, 1,2}^{0,0:2,1, \dots, 2,1} \left[\begin{array}{c} y \\ \vdots \\ y \end{array} \middle| \begin{array}{l} -(1, 1); \dots; (1, 1) \\ (0; 1, \dots, 1): (k_1 + 1, \frac{1}{2}), (t_1 + 1, \frac{1}{2}); \dots; (k_N + 1, \frac{1}{2}), (t_N + 1, \frac{1}{2}) \end{array} \right].$$

The asymptotic expansions of $\Theta(y)$ when $y \rightarrow \infty$ can be obtained by computing the residue of the multivariable Fox's H function by using [49, eq. (1.5.9)] as $\Theta(y) \approx \prod_{i=1}^N \Gamma(k_i + 1) \Gamma(t_i + 1)$. Moreover, by recognizing that

$$\sum_{k_1, \dots, k_N=0}^{\infty} \sum_{t_1, \dots, t_N=0}^{\infty} \prod_{i=1}^N \frac{e^{-K^h} K^{h k_i}}{\Gamma(k_i + 1)} \frac{e^{-K^g} K^{g t_i}}{\Gamma(t_i + 1)} = 1, \quad (10)$$

$$\mathbf{H}_{p,q:p_1, q_1, \dots, p_r, q_r}^{0, n: m_1, n_1, \dots, m_r, n_r} \left[\begin{array}{c} z_1 \\ \vdots \\ z_r \end{array} \middle| \begin{array}{l} (a_j; \alpha_j^{(1)}, \dots, \alpha_j^{(r)})_{1:p} : (c_j^{(1)}, \gamma_j^{(1)})_{1,p_1}; \dots; (c_j^{(r)}, \gamma_j^{(r)})_{1,p_r} \\ (b_j; \beta_j^{(1)}, \dots, \beta_j^{(r)})_{1:q} : (d_j^{(1)}, \delta_j^{(1)})_{1,q_1}; \dots; (d_j^{(r)}, \delta_j^{(r)})_{1,q_r} \end{array} \right] \\ = \frac{1}{(2\pi j)^r} \int_{\mathcal{L}_1} \dots \int_{\mathcal{L}_r} \Psi(\xi_1, \dots, \xi_r) \left\{ \prod_{i=1}^r \phi_i(\xi_i) z_i^{\xi_i} \right\} d_{\xi_1} \dots d_{\xi_r} \quad (7)$$

where $j = \sqrt{-1}$,

$$\phi_i(\xi_i) = \frac{\prod_{k=1}^{m_i} \Gamma(d_k^{(i)} + \xi_i \delta_k^{(i)}) \prod_{j=1}^{n_i} \Gamma(1 - c_j^{(i)} - \xi_i \gamma_j^{(i)})}{\prod_{k=m_i+1}^{q_i} \Gamma(1 - d_k^{(i)} - \xi_i \delta_k^{(i)}) \prod_{j=n_i+1}^{p_i} \Gamma(c_j^{(i)} + \xi_i \gamma_j^{(i)})}$$

and

$$\Psi(z_1, \dots, z_r) = \frac{\prod_{j=1}^n \Gamma(1 - a_j + \sum_{i=1}^r \alpha_j^{(i)} \xi_i)}{\prod_{j=n+1}^p \Gamma(a_j + \sum_{i=1}^r \alpha_j^{(i)} \xi_i) \prod_{j=1}^q \Gamma(1 - b_j + \sum_{i=1}^r \beta_j^{(i)} \xi_i)}$$

TABLE 2. Minimum required terms and truncation error for different parameters K^h, K^g, N .

Parameters	$\mathcal{E}(M)$	M
$N = 2, K^h = 1, K^g = 2$	6.2110^{-6}	20
$N = 3, K^h = 1, K^g = 1$	7.0310^{-6}	24
$N = 3, K^h = 2, K^g = 3$	8.1910^{-6}	21
$N = 5, K^h = 1, K^g = 2$	8.4510^{-6}	26

the truncation error $\mathcal{E}(M)$ can be simplified as

$$\mathcal{E}(M) = 1 - \sum_{k_1, \dots, k_N=0}^M \sum_{t_1, \dots, t_N=0}^M \prod_{i=1}^N \frac{e^{-K^h k_i} K^{h k_i} e^{-K^g t_i} K^{g t_i}}{\Gamma(k_i + 1) \Gamma(t_i + 1)}. \quad (11)$$

Hence, it can be shown that $\mathcal{E}(M) \rightarrow 0$ when $M \rightarrow \infty$.

To demonstrate the convergence of the series in (11), Table 2 depicts the required truncation terms for different system and channel parameters. With a satisfactory accuracy (e.g., smaller than 10^{-5}), only less than 30 terms are needed, regardless of the average SNR, the number of RIS elements and the Rician factor, for all considered cases. ■

Remark 1: The derived analytical expressions for the outage probability in (4) and (8) are general and new, and can be easily mapped into most existing fading models. The obtained analytical frameworks are, to the best of our knowledge, the first ones in the literature that yield the exact end-to-end SNR distribution of an RIS-assisted systems in terms of the multivariate Fox’s H-function. This is in contrast with the recently reported expressions in [3, eqs. (4), (7)] and [16, eq. (17)], which are based on approximations (the CLT in [3] and the moment-based Gamma approximation in [16]), in order to overcome the intricacy of the exact statistical modeling of the end-to-end SNR in RIS-aided systems. The novelty of the proposed approach is also apparent from the summary given in Table 1. For the convenience of the readers, Table 3 provides the explicit expression of the outage probability for several widely used fading distributions. Notably, the outage expressions in Table 3 are evaluated by using the efficient Python implementation code for the multivariable Fox’s H function presented in [46]. We also used an efficient GPU-oriented MATLAB routine for the multivariate Fox’s H-function evaluation introduced in [47].

A. DIVERSITY ORDER AND CODING GAIN

In this section, we analyze the diversity order and coding gain of RIS-assisted communications over generalized fading channels. In the current literature, the diversity order has been assessed by relying on approximations and bounds [15]–[26] (see Table 1), and under Rayleigh fading. A common approach for analyzing the diversity order of RIS-aided systems is to leverage the CLT. However, this approach is accurate only for a large number of reconfigurable elements [3], and, in general, it is not sufficiently accurate for high-SNR analysis, which is the regime of interest for analyzing the diversity order [19]. In [15], for example, the

diversity order was shown to be $\frac{N}{2} \frac{\pi^2}{16 - \pi^2}$ in Rayleigh fading, which implies that the full diversity order cannot be obtained even in the absence of phase errors. By resorting to some bounds, however, the authors of [19] recently showed that the full diversity order equal to N is achievable in Rayleigh fading (even in the presence of phase errors). A detailed summary of the current methods and results on the diversity order of RIS-aided systems is available in Table 1.

In what follows, building upon the high-SNR analysis of the exact outage probability in Proposition 1 and Proposition 2, we compute the exact diversity order and coding gain of RIS-assisted systems over generalized fading. We prove, in particular, that the diversity order in Rayleigh fading is N and that it may exceed this value in less severe fading channels.

Proposition 3: Consider the multivariate Fox’s H-function in (4) and define the set of poles $\mathcal{S} = (\zeta_1, \dots, \zeta_N)$, where $\zeta_l = \min_{j=1, \dots, \tilde{m}_l} \{ \frac{\xi_{jl}}{\Xi_{jl}}, \dots, \frac{\xi_{\tilde{m}_l j}}{\Xi_{\tilde{m}_l j}} \}$. For each pole ξ_j , define the set of indexes $K_j^{(l)} = \{k : k \in \{1, \dots, \tilde{m}_l\}, r_{k,j} = -\xi_l k + \Xi_{lk} \frac{\xi_{jl}}{\Xi_{jl}} \in \{0, 1, 2, \dots\}\}$ and let $\tilde{N}_j^{(l)} = |K_j^{(l)}|$ be the multiplicity of the pole ζ_l with $j_l = \arg \min_{j=1, \dots, \tilde{m}_l} \{ \xi_{jl} / \Xi_{jl} \}$. The asymptotic expansion of (4) near $\rho_t = \frac{\gamma_{th}}{\rho} = 0$ is [49, Th. 1.2]

$$\Pi(\rho, N) \approx \frac{\tau}{\Gamma(1 + \sum_{l=1}^N \zeta_l)} \prod_{l=1}^N \tilde{\Theta}_l(-\zeta_l) \left[\ln \left(\sqrt{\frac{\rho}{\tilde{c}_l \gamma_{th}}} \right) \right]^{\tilde{N}_{j_l}^{(l)} - 1} \tilde{c}_l^{\zeta_l} \left(\frac{\gamma_{th}}{\rho} \right)^{\frac{\zeta_l}{2}}, \quad (12)$$

where the constants $\tilde{\Theta}_l, l = 1, \dots, N$, are given by

$$\tilde{\Theta}_l(\zeta_l) = \frac{1}{\Gamma(\tilde{N}_{j_l}^{(l)})} \prod_{k=1}^{\tilde{N}_{j_l}^{(l)}} \frac{(-1)^{j_k}}{j_k! \Xi_k} \frac{\prod_{i \notin K_{j_l}^{(l)}} \Gamma(\xi_i + \Xi_i \zeta_l) \prod_{i=1}^{\tilde{m}_l} \Gamma(1 - \delta_i - \Delta_i \zeta_l)}{\prod_{i=\tilde{m}_l+1}^{\tilde{p}_l} \Gamma(\delta_i + \Delta_i \zeta_l) \prod_{i=\tilde{m}_l+1}^{\tilde{q}_l} \Gamma(1 - \xi_i - \Xi_i \zeta_l)}. \quad (13)$$

Proof: Equation (12) is obtained by evaluating the residues of the Mellin-Barnes integrals in (34) at the poles of the terms $\Gamma(\xi_j + u_l \Xi_{lj}), j = 1, \dots, \tilde{m}_l$, according to [49, Th. 1.2] and by keeping only the dominant terms using [49, eq. (1.8.3)].

As mentioned, the Fox’s H-function fading distribution generalizes many well-known fading distributions, such as the Rayleigh, Nakagami- m , and α - μ distributions. It is interesting to analyze how the general expressions derived for the asymptotic outage probability simplify when selecting the parameters corresponding to known distributions. We have three possible scenarios.

- Scenario 1: The poles $\frac{\xi_{jl}}{\Xi_{jl}}, j = 1, \dots, \tilde{m}_l$ are simple. This occurs when $r_{k_{j_l}}$ is neither a positive integer nor zero. In this case $\tilde{N}_{j_l}^{(l)} = 1$. This case study applies, for instance, to i.n.i.d. h_i and g_i over Nakagami- m and i.n.i.d. α - μ , with $\alpha_i^h \mu_i^h \neq \alpha_i^g \mu_i^g$, fading channels.

TABLE 3. Outage probability of RIS-assisted systems over widely used fading channel models.

Instantaneous Fading Distribution	Outage Probability $\Pi(\rho, N)$
Nakagami- m Fading [48, Table IV]: $f_{ y_i }(x) = \frac{\sqrt{m_i^y}}{\Gamma(m_i^y)} H_{0,1}^{1,0} \left[\sqrt{m_i^y} x \mid (m_i^y - \frac{1}{2}, \frac{1}{2}) \right]$	$\Pi(\rho, N) = \left(\prod_{i=1}^N \Gamma(m_i^h) \Gamma(m_i^g) \right)^{-1}$ $\times H_{0,1:1,2,\dots,1,2}^{0,0:2,1,\dots,2,1} \left[\begin{array}{c} \sqrt{m_1^h m_1^g} \sqrt{\rho t} \\ \vdots \\ \sqrt{m_N^h m_N^g} \sqrt{\rho t} \end{array} \mid \begin{array}{c} - : (1, 1), -; \dots; (1, 1), - \\ (0; 1, \dots, 1) : \{\xi_1, \Xi_1\}; \dots; \{\xi_N, \Xi_N\} \end{array} \right]$ $\{\xi_i, \Xi_i\} = (m_i^h, \frac{1}{2}), (m_i^g, \frac{1}{2})$
α - μ Fading [48, Table IV]: $f_{ y_i }(x) = \frac{\sqrt{\eta_i^y}}{\Gamma(\mu_i^y)} H_{0,1}^{1,0} \left[\sqrt{\eta_i^y} x \mid (\mu_i^y - \frac{1}{\alpha_i^y}, \frac{1}{\alpha_i^y}) \right]$ where $\eta_i^y = \frac{\Gamma(\mu_i^y + \frac{2}{\alpha_i^y})}{\Gamma(\mu_i^y)}$	$\Pi(\rho, N) = \left(\prod_{i=1}^N \Gamma(\mu_i^h) \Gamma(\mu_i^g) \right)^{-1}$ $\times H_{0,1:1,2,\dots,1,2}^{0,0:2,1,\dots,2,1} \left[\begin{array}{c} \sqrt{\eta_1^h \eta_1^g} \sqrt{\rho t} \\ \vdots \\ \sqrt{\eta_N^h \eta_N^g} \sqrt{\rho t} \end{array} \mid \begin{array}{c} - : (1, 1), -; \dots; (1, 1), - \\ (0; 1, \dots, 1) : \{\xi_1, \Xi_1\}; \dots; \{\xi_N, \Xi_N\} \end{array} \right]$ $\{\xi_i, \Xi_i\} = (\mu_i^h, \frac{1}{\alpha_i^h}), (\mu_i^g, \frac{1}{\alpha_i^g})$
Rice Fading [48, Eq. (2.16)] $f_{ y_i }(x) = \lim_{K \rightarrow \infty} \sum_{k=0}^K \kappa_k^y H_{0,1}^{1,0} \left[c_k^y z \mid (k + \frac{1}{2}, \frac{1}{2}) \right]$	$\Pi(\rho, N) = \sum_{k_1, \dots, k_N=0}^{\infty} \sum_{t_1, \dots, t_N=0}^{\infty} \tau H_{0,1:1,2,\dots,1,2}^{0,0:2,1,\dots,2,1}$ $\left[\begin{array}{c} \Delta \sqrt{\rho t} \\ \vdots \\ \Delta \sqrt{\rho t} \end{array} \mid \begin{array}{c} - : (1, 1); \dots; (1, 1) \\ (0; 1, \dots, 1) : (k_1 + 1, \frac{1}{2}), (t_1 + 1, \frac{1}{2}); \dots; (k_N + 1, \frac{1}{2}), (t_N + 1, \frac{1}{2}) \end{array} \right]$
Fisher-Snedecor \mathcal{F} [44]: $f_{ y_i }(x) = \frac{m_i^y}{m_{s_i}^y \Gamma(m_{s_i}^y) \Gamma(m_i^y)} \times H_{1,1}^{1,1} \left[\frac{m_i^y x}{m_{s_i}^y} \mid (m_i^y - \frac{1}{2}, \frac{1}{2}) \right]$	$\Pi(\rho, N) = \left(\prod_{i=1}^N \Gamma(m_{s_i}^g) \Gamma(m_i^g) \Gamma(m_{s_i}^h) \Gamma(m_i^h) \right)^{-1}$ $\times H_{0,1:3,2,\dots,3,2}^{0,0:2,3,\dots,2,3} \left[\begin{array}{c} \sqrt{\frac{m_i^h m_i^g}{m_{s_i}^h m_{s_i}^g}} \sqrt{\rho t} \\ \vdots \\ \sqrt{\frac{m_N^h m_N^g}{m_{s_N}^h m_{s_N}^g}} \sqrt{\rho t} \end{array} \mid \begin{array}{c} - : (1, 1), \{\delta_1, \Delta_1\}; \dots; (1, 1), \{\delta_N, \Delta_N\} \\ (0; 1, \dots, 1) : \{\xi_1, \Xi_1\}; \dots; \{\xi_N, \Xi_N\} \end{array} \right]$ $\{\delta_i, \Delta_i\} = (1 - m_{s_i}^h, \frac{1}{2}), (1 - m_{s_i}^g, \frac{1}{2})$ $\{\xi_i, \Xi_i\} = (m_i^h, \frac{1}{2}), (m_i^g, \frac{1}{2})$
Generalized \mathcal{K} [48, Table IV]: $f_{ y_i }(x) = \frac{\sqrt{\kappa_i^y}}{\Gamma(m_i^y) \Gamma(k_i^y)} \times H_{0,2}^{2,0} \left[x \sqrt{m_i^y \kappa_i^y} \mid (m_i^y - \frac{1}{2}, \frac{1}{2}), (k_i^y - \frac{1}{2}, \frac{1}{2}) \right]$	$\Pi(\rho, N) = \left(\prod_{i=1}^N \Gamma(m_i^h) \Gamma(\kappa_i^h) \Gamma(m_i^g) \Gamma(\kappa_i^g) \right)^{-1}$ $\times H_{0,1:1,4,\dots,1,4}^{0,0:4,1,\dots,4,1} \left[\begin{array}{c} \sqrt{m_1^h \kappa_1^h m_1^g \kappa_1^g} \sqrt{\rho t} \\ \vdots \\ \sqrt{m_N^h \kappa_N^h m_N^g \kappa_N^g} \sqrt{\rho t} \end{array} \mid \begin{array}{c} - : (1, 1), -; \dots; (1, 1), - \\ (0; 1, \dots, 1) : (\xi_1, \Xi_1)_{p_{11}}; \dots; (\xi_N, \Xi_N)_{p_{N1}} \end{array} \right]$ $\{\xi_i, \Xi_i\} = (m_i^h, \frac{1}{2}), (m_i^g, \frac{1}{2}), (k_i^h, \frac{1}{2}), (k_i^g, \frac{1}{2})$

- Scenario 2: The poles $\frac{\xi_{jl}}{\Xi_{lj}}, j = 1, \dots, \tilde{m}_l$, all coincide. This occurs when $\frac{\xi_{jl}}{\Xi_{lj}} = \frac{\xi_{lk}}{\Xi_{lk}}, k, j = 1, \dots, \tilde{m}_l$, and in this case $\tilde{N}_{jl}^{(l)} = \tilde{m}_l$. This case study includes, as special cases, Rayleigh, i.i.d. Nakagami- m , and α - μ , with $\alpha_i^h \mu_i^h = \alpha_i^g \mu_i^g$, fading channels, for which $\tilde{N}_{jl}^{(l)} = 2$.
- Scenario 3: Some poles are simple and the others coincide, such that r_{kjl} is a positive integer. This case study, however, does not apply to (12), since only the smallest pole (the dominant pole), i.e., $j_l = \arg \min_{j=1, \dots, \tilde{m}_l} \{\xi_{lj} / \Xi_{lj}\}$, is considered in (12).

Taking into consideration the just mentioned scenarios, the diversity order and the coding gain of RIS-assisted systems

over generalized fading channels is stated in the following proposition. ■

Proposition 4: Consider the general Fox's-H fading model in (2). The asymptotic (for high-SNR) outage probability of an RIS-aided system can be formulated as

$$\Pi(\rho, N) \underset{\rho \rightarrow \infty}{\approx} (\mathcal{G}_d \rho)^{-\mathcal{G}_d}, \tag{14}$$

where \mathcal{G}_d denotes the diversity order given by

$$\mathcal{G}_d = \frac{\sum_{i=1}^N \min_{j=1, \dots, \tilde{m}_l} \left\{ \frac{\xi_{ij}}{\Xi_{ij}} \right\}}{2}, \tag{15}$$

TABLE 4. Diversity and coding gain of RIS-assisted systems over widely used fading channels.

Distribution	Diversity Order	Coding Gain
Rayleigh	N	$\frac{1}{\gamma_{th}} \left(-\ln \left(\frac{\gamma_{th}}{\rho} \right)^N \frac{2^N}{\Gamma(1+2N)} \right)^{-\frac{1}{N}}$
i.i.d. Nak.- m	$\sum_{i=1}^N \min\{m_i^h, m_i^g\}$	$\frac{1}{\gamma_{th}} \left(\frac{2^N \prod_{j=1}^N (m_j^h m_j^g)^{\min\{m_j^h, m_j^g\}} \Gamma \left(m_j^{\arg \min\{m_j^h, m_j^g\}} \right)}{\left(\prod_{i=1}^N \Gamma(m_i^h) \Gamma(m_i^g) \right) \Gamma(1+2 \sum_{i=1}^N \min\{m_i^h, m_i^g\})} \right)^{\frac{1}{\sum_{i=1}^N \min\{m_i^h, m_i^g\}}}$
i.i.d. α - μ	$\frac{\sum_{i=1}^N \min\{\alpha_i^h \mu_i^h, \alpha_i^g \mu_i^g\}}{2}$	$\frac{1}{\gamma_{th}} \left(\frac{\prod_{j=1}^N \alpha_j^{\arg \min\{\alpha_j^h \mu_j^h, \alpha_j^g \mu_j^g\}} \Gamma \left(\mu_j^{\arg \min\{\alpha_j^h \mu_j^h, \alpha_j^g \mu_j^g\}} \right)}{\prod_{j=1}^N \left(\left(\sqrt{\eta_j^h \eta_j^g} \right)^{-\min\{\alpha_j^h \mu_j^h, \alpha_j^g \mu_j^g\}} \Gamma(\mu_j^h) \Gamma(\mu_j^g) \right) \Gamma(1+\sum_{i=1}^N \min\{\alpha_i^h \mu_i^h, \alpha_i^g \mu_i^g\})} \right)^{\frac{2}{\sum_{i=1}^N \min\{\alpha_i^h \mu_i^h, \alpha_i^g \mu_i^g\}}}$
Rice	N	$\frac{1}{\gamma_{th}} \frac{e^{(K^h+K^g)} \left(-\ln \left(\frac{\Delta^2 \gamma_{th}}{\rho} \right)^{-1} \right) \Gamma(1+2N)^{\frac{1}{N}}}{2(1+K^h)(1+K^g)}$

and \mathcal{G}_c denotes that coding gain given by

$$\mathcal{G}_c = \begin{cases} \frac{1}{\gamma_{th}} \left(\frac{\tau \left(\prod_{i=1}^N \tilde{\Theta}_i(-\zeta_i) \tilde{\zeta}_i^{\zeta_i} \right)}{\Gamma(1+\sum_{i=1}^N \zeta_i)} \right)^{-\frac{2}{\sum_{i=1}^N \zeta_i}} & \text{Scenario 1,} \\ \frac{1}{\gamma_{th}} \left(\frac{\tau \left(\prod_{i=1}^N \tilde{\Theta}_i(-\zeta_i) \ln \left(\frac{\rho \tilde{\zeta}_i}{\gamma_{th}} \right) \tilde{\zeta}_i^{\zeta_i} \right)}{\Gamma(1+\sum_{i=1}^N \zeta_i)} \right)^{-\frac{2}{\sum_{i=1}^N \zeta_i}} & \text{Scenario 2,} \end{cases} \quad (16)$$

where $\zeta_l = \min_{j=1, \dots, \tilde{m}_l} \{\xi_{lj} / \Xi_{lj}\}$, and the constants $\tilde{\Theta}_l(\zeta_l)$ are given in Proposition 3 with $\tilde{N}_{jl}^{(l)} = 1$ and $\tilde{N}_{jl}^{(l)} = 2$ for Scenario 1 and 2, respectively.

Proof: It follows from Proposition 3, under the assumptions stated in Scenarios 1 and 2. ■

Remark 2: The usually considered Rayleigh fading channel model (see Table 4) can be retrieved from Proposition 4 by considering Scenario 2 with $\zeta_l = 2$ for $l = 1, \dots, N$.

Proposition 5: Consider an RIS-assisted communication system over Rician fading. From (8), the asymptotic outage probability is

$$\Pi(\rho, N) \approx \frac{2^N (1+K^h)^N (1+K^g)^N}{\Gamma(1+2N)} e^{-N(K^h+K^g)} \ln \left(\frac{\rho}{\Delta^2 \gamma_{th}} \right)^N \left(\frac{\rho}{\gamma_{th}} \right)^{-N}. \quad (17)$$

Proof: It follows by computing the residues at $\zeta_l = \min\{2k_l + 2, 2t_l + 2\}$, $l = 1, \dots, N$, and by keeping only the dominant term of the infinite series expansion in (8), which corresponds to $k_l = t_l = 0$. Then, steps similar to Proposition 3 yield (17) with the aid of some manipulations. ■

By substituting the specific parameters of the fading models summarized in Table 2 into the generalized expressions of the outage probability in Propositions 4 and 5 (under the assumptions of Scenarios 1 and 2), it is possible to obtain explicit expressions for the corresponding diversity order \mathcal{G}_d and coding gain \mathcal{G}_c . These are reported in Table 4, from which the following important conclusions and performance trends are unveiled.

- Over Rayleigh fading channels, the obtained results coincide with those derived in earlier research works as reported in Table 1, but by using different methods of analysis, e.g., approximations and bounds.
- RIS-aided systems achieve a diversity order equal to N for an arbitrary number N of reconfigurable elements in both Rayleigh and Rice fading. The impact of the LoS component, i.e., K , is mainly reflected in the achievable coding gain. In particular, a strong LoS component (large K) is beneficial.
- Under severe fading $m_i^h, m_i^g < 1$ or $\alpha_i^h \mu_i^h, \alpha_i^g \mu_i^g < 1$, RIS-aided systems achieve a diversity order less than N . However, such a scenario may not occur in optimized deployments in which the RISs are positioned in order to leverage the LoS paths with the transmitter and possibly with the receiver. In these cases, m_i^h and m_i^g are, in fact, relatively large.
- Under fading channels less severe than Rayleigh, e.g., m_i^h and m_i^g are larger than one, a diversity order greater than N can be obtained.
- Under the assumption of Scenario 2, which encompasses i.i.d. Rayleigh fading, the scaling law of the outage probability as a function of $\rho \rightarrow \infty$ is $(\ln(\rho)/\rho)^N$. This trend is in agreement with [16], where it was proved by using exact analysis for $N = 1$ and upper and lower bounds for $N > 1$. Similar trends were reported in [19]. It is worth noting that this scaling law holds true for Rice fading as well, as unveiled, for the first time in the literature, by (17). As remarked in [16], this is a new scaling law, which generalizes the definitions of diversity order and coding gain typically used in wireless communications [36].
- Under the assumptions of Scenario 1 (e.g., i.i.d. Nakagami- m and α - μ fading in Table 4), the scaling law $(\ln(\rho)/\rho)^N$ does not emerge, and the outage probability scales as ρ^{-N} for $\rho \rightarrow \infty$. To the best of the authors' knowledge, this difference in the scaling law between Scenario 1 and Scenarios 2 was never reported in the literature.

IV. OUTAGE PROBABILITY - WITH PHASE NOISE

In practice, the phase shifts of the reconfigurable elements of an RIS cannot be optimized with an arbitrary precision, e.g., because of the finite number of quantization bits used or because of errors when estimating the phases of the fading channels [18], [20]. In these cases, the phase of the i th element of the RIS can be written as $\phi_i = -\angle h_i - \angle g_i + \theta_i$, where θ_i denotes a random phase noise, which is assumed to be i.i.d. in this paper. Thus, the equivalent channel observed by the receiver is a complex random variable and the SNR is

$$\gamma = \rho \left| \sum_{i=1}^N |h_i| |g_i| e^{j\theta_i} \right|^2 = \rho |H|^2. \quad (18)$$

We assume that the distribution of θ_i is arbitrary but its mean is zero. Examples of phase noise distributions include Gaussian, generalized uniform, and uniform RVs whose characteristic functions, $\mathbb{E}\{e^{j\theta}\} = \mathcal{K}_t$, are as follows:

- 1) Gaussian $\theta_i \sim \mathcal{N}(0, \sigma^2)$ [50]

$$\mathcal{K}_t \stackrel{(a)}{\approx} e^{-\sigma^2 \frac{t^2}{2}}, \quad (19)$$

- 2) Generalized uniform $\theta_i \sim \mathcal{U}(-q\pi, q\pi)$, $q \neq 1$, [20]

$$\mathcal{K}_t = \frac{\sin(q\pi t)}{q\pi t}, \quad (20)$$

- 3) Uniform $\theta_i \sim \mathcal{U}(-\pi, \pi)$ [20]

$$\mathcal{K}_t = \frac{\sin(\pi t)}{\pi t}, \quad (21)$$

where (a) follows from $\mathbb{E}\{e^{j\theta_i}\}_{\theta_i \in [\pi, \pi]} \approx \mathbb{E}\{e^{j\theta_i}\}_{\theta_i \in [-\infty, \infty]}$, $\sigma^2 \ll 1$, which stems from the fact that, in practice, we are interested in standard deviations of only a few degrees.

It is worth noting that the Gaussian distribution is versatile to represent continuous phase errors. In [50], e.g., it was shown that the phase errors are Gaussian distributed under widely applicable assumptions. Likewise, due to hardware limitations, only a finite number of phase shifts can be realized, which leads to quantization errors. In this case, the generalized uniform distribution constitutes a versatile model to account for the quantization noise by setting $q = 2^{-L}$, where $L \geq 1$ is a positive integer that denotes the number of quantization bits used [18], [20].

The SNR in (18) is formulated in terms of the square magnitude of a linear combination of complex random variables with random magnitudes and random phases. In general, the calculation of the exact distribution of the SNR in (18) is

an open research issue, and is very intricate for arbitrary values of N . To tackle this issue, we proceed as follows: (i) first, we study the distribution of the SNR in (18) under the assumption of a large number of reconfigurable elements N of the RIS, i.e., $N \gg 1$. The obtained analytical framework is based on the CLT and is typically appropriate for analyzing RIS-aided systems with practical numbers of reconfigurable elements and for typical values of ρ . As noted in, e.g., [19], the resulting analysis is usually not accurate in the high-SNR regime (i.e., for $\rho \rightarrow \infty$), and, therefore, for analyzing the attainable diversity order; and (ii) then, we introduce upper and lower bounds for the SNR in (18) in the presence of phase noise. The objective is to identify sufficient conditions for achieving the full diversity order. The main peculiarity of the latter approach lies in its applicability to RIS-aided systems with an arbitrary number of reconfigurable elements N and for any SNR regime.

A. PERFORMANCE ANALYSIS FOR LARGE N AND FINITE VALUES OF ρ

In this sub-section, we introduce an analytical framework for computing the outage probability of RIS-aided systems in the presence of phase noise and under the assumption $N \gg 1$.

Proposition 6: Define $\Lambda_1 = \mathbb{E}\{|h_i|\}$ and $\Lambda_2 = \mathbb{E}\{|g_i|\}$. For large values of N , the outage probability in the presence of phase noise can be formulated as follows.

- Case 1: In the presence of Gaussian and generalized uniform phase noise, we have (22), shown at the bottom of this page, where $\mathcal{B} = \{(1; -1, -1, -1), (\frac{1}{2}; -1, 0, -1), (1; 0, -1, -1)\}$, $\nu = \mathcal{K}_1 \Lambda_1 \Lambda_2$, $\sigma_Y^2 = \frac{1}{2N}(1 - \mathcal{K}_2)$, and $\sigma_X^2 = \frac{1}{2N}(1 + \mathcal{K}_2 - 2\mathcal{K}_1^2 \Lambda_1^2 \Lambda_2^2)$.
- Case 2: In the presence of uniform phase noise, the outage probability is obtained as shown in (23) at the bottom of this page.

Proof: The proof is based on the application of the CLT. See Appendix A. ■

To the best of our knowledge, Proposition 6 is a new result that is not available in the literature and is applicable to generalized fading distributions in the presence of phase noise.

B. DIVERSITY ANALYSIS FOR LARGE N

Based on Proposition 6, this sub-section studies the outage probability in the high-SNR regime, i.e., for $\rho \rightarrow \infty$. It is

$$\Pi(\rho, N) = \frac{1}{2\pi} \mathbf{H}_{3,1;1,1;2,1}^{0,2;1,1;1,1;2,1} \left[\begin{array}{c} \frac{-\gamma th}{N^2 4\nu^2 \rho} \\ \frac{\gamma th}{N^2 \nu^2 \rho} \\ \frac{\gamma th}{N^2 \nu^2 \rho} \end{array} \middle| \begin{array}{c} \mathcal{B}; (0, 2); (1, 1), \left(\frac{\nu^2}{2\sigma_X^2}, 2\right); (1, 1), \left(\frac{\nu^2}{2\sigma_Y^2}, 2\right) \\ (1; 0, -1, -1); (0, 1); \left(\frac{\nu^2}{2\sigma_X^2}, 1\right); \left(\frac{\nu^2}{2\sigma_Y^2}, 1\right), \left(\frac{1}{2}, 1\right) \end{array} \right] \quad (22)$$

$$\Pi(\rho, N) = \pi^{-1} \mathbf{H}_{0,1;2,2;2,2}^{0,0;2,1;2,1} \left[\begin{array}{c} \frac{\gamma th}{N^2 \rho} \\ \frac{\gamma th}{N^2 \rho} \end{array} \middle| \begin{array}{c} - : (N, 2), (1, 1); (N, 2), (1, 1) \\ (0; 1, 1) : (N, 1), \left(\frac{1}{2}, 1\right); (N, 1), \left(\frac{1}{2}, 1\right) \end{array} \right] \quad (23)$$

known, however, that the CLT may not be suitable for analyzing the outage probability for $\rho \rightarrow \infty$ if N is fixed. The analysis of this sub-section serves, therefore, as a benchmark for better understanding the limitations of the CLT when applied to RIS-aided systems when analyzing their performance in the high-SNR regime. This is elaborated next.

Proposition 7: Assume $\rho \rightarrow \infty$. Based on Proposition 6, the asymptotic outage probability in the presence of phase noise can be formulated as

$$\Pi(\rho, N) \underset{\rho \rightarrow \infty}{\approx} \begin{cases} \mathcal{A}_G \left(\frac{\rho}{\gamma_{th}} \right)^{-\left(\frac{v^2}{2\sigma_X^2} + \frac{1}{2} \right)} & \text{Case 1,} \\ \frac{\Gamma(N - \frac{1}{2})}{\Gamma(N)^2} \left(\frac{\rho}{\gamma_{th}} \right)^{-1} & \text{Case 2,} \end{cases} \quad (24)$$

where

$$\mathcal{A}_G = \frac{(N^2 v^2)^{-\left(\frac{v^2}{2\sigma_X^2} + \frac{1}{2} \right)}}{\sqrt{\pi}} \sqrt{\frac{v^2 \Gamma\left(\frac{1}{2} - \frac{v^2}{2\sigma_X^2}\right)}{2\sigma_Y^2 \Gamma\left(\frac{3}{2} + \frac{v^2}{2\sigma_X^2}\right)}}. \quad (25)$$

Proof: Equation (24) is obtained by computing the residues of the integrand in (43) and (45) by using [49, eqs. (1.84), (1.85)]. As for Case 1, the residue is computed at the points $u_1 = \frac{v^2}{2\sigma_X^2}$, $u_2 = \min\{\frac{v^2}{2\sigma_Y^2}, \frac{1}{2}\} = \frac{1}{2}$, and $u_3 = 0$. As for Case 2, the residue is computed at $(u_1, u_2) = (\frac{1}{2}, \frac{1}{2})$.

From (24), we evince that the diversity order based on the CLT approximation for $N \gg 1$ is

$$\mathcal{G}_d^{\text{CLT}} = \begin{cases} N\mathcal{E} + \frac{1}{2} & \text{Case 1,} \\ 1 & \text{Case 2,} \end{cases} \quad (26)$$

where $\mathcal{E} = (\mathcal{K}_1 \Lambda_1 \Lambda_2)^2 / (1 + \mathcal{K}_2 - 2\mathcal{K}_1^2 \Lambda_1^2 \Lambda_2^2)$. ■

Remark 3: Based on (26), we conclude that, in general, the diversity order in the presence of phase noise is less than the full diversity order that is achievable in the absence of phase noise, which is given in (15). As a case study, let us consider that the phase noise originates from the quantization bits L used for the phase shifts. From (26), we obtain $\mathcal{E} = \frac{1}{2}$ for $L = 1$ and $\mathcal{E} < 1$ for $L > 1$. Over Rayleigh fading, in particular, we obtain $\mathcal{G}_d^{\text{CLT}} \approx 0.78N + 0.5$ if $L = 2$ and $\mathcal{G}_d^{\text{CLT}} \approx 0.8N + 0.5$ if $L \rightarrow \infty$ (i.e., no phase noise). Therefore, we evince that $\mathcal{G}_d^{\text{CLT}} < \mathcal{G}_d$ for finite and infinite values of L , which is in disagreement with (15) in the absence of phase noise (i.e., $L \rightarrow \infty$).

The example in Remark 3 confirms the unsuitability of the CLT for high-SNR analysis, and, in particular, for estimating the diversity order of RIS-assisted systems. To further corroborate the statements in Remark 4, let us assume $N = 1$ in (18). In this case, we would have $\gamma(N = 1) = \rho(|h_1||g_1|\cos(\theta_1))^2 + \rho(|h_1||g_1|\sin(\theta_1))^2 = \rho|h_1|^2|g_1|^2$, which implies that the SNR is independent of the phase error. This is different from (26).

In the next sub-section, we introduce sufficient conditions for ensuring that the full diversity order is achieved in RIS-assisted communications impaired by phase noise.

C. DIVERSITY ANALYSIS FOR ARBITRARY N

The analytical framework introduced in the previous section based on the CLT is usually accurate for analyzing the performance of RIS-assisted communications for practical values of N and for typical values of the SNR. However, it is not sufficiently accurate for estimating the diversity order, i.e., for $\rho \rightarrow \infty$. In the present paper, for these reasons, we do not attempt to introduce approximated analytical frameworks but focus our attention on identifying sufficient conditions for guaranteeing that RIS-aided systems achieve the full diversity order even in the presence of phase noise. This is a fundamental open issue for designing and optimizing RIS-aided systems. For example, the approach introduced in this section allows us to identify the minimum number of quantization bits that are needed for ensuring no diversity loss. This specific problem has been recently analyzed in [19], where it is shown that, under i.i.d. Rayleigh fading, two quantization bits (i.e., $L = 2$) are necessary. The approach proposed in [19] is specifically tailored for analyzing the impact of quantization bits in the presence of i.i.d. Rayleigh fading. The analytical approach proposed in this section, on the other hand, is applicable to arbitrary distributions for the channel fading and for the phase noise.

To this end, we re-write the end-to-end SNR in (18) as $\gamma = \rho|H|^2 = \rho(X^2 + Y^2)$, where $X = \sum_{i=1}^N |h_i||g_i|\cos(\theta_i)$ and $Y = \sum_{i=1}^N |h_i||g_i|\sin(\theta_i)$. Also, we define $\varepsilon_{\min} = \min_{n \neq m \in [1, N]} \{\cos(\theta_n - \theta_m)\}$. The main results are stated in the following two propositions.

Proposition 8: Assume $\varepsilon_{\min} = \min_{n \neq m \in [1, N]} \{\cos(\theta_n - \theta_m)\} \geq 0$. The SNR in (18) is upper and lower bounded as follows

$$\rho \sum_{i=1}^N |h_i|^2 |g_i|^2 \leq \rho(X^2 + Y^2) \leq \rho \left(\sum_{i=1}^N |h_i||g_i| \right)^2. \quad (27)$$

Proof: Be definition, we have

$$\begin{aligned} X^2 &= \sum_{n=1}^N |h_n|^2 |g_n|^2 \cos^2(\theta_n) \\ &+ \sum_{n=1}^N \sum_{m \neq n=1}^N (|h_n||g_n|\cos(\theta_n))(|h_m||g_m|\cos(\theta_m)), \end{aligned} \quad (28)$$

and

$$\begin{aligned} Y^2 &= \sum_{n=1}^N |h_n|^2 |g_n|^2 \sin^2(\theta_n) \\ &+ \sum_{n=1}^N \sum_{m \neq n=1}^N (|h_n||g_n|\sin(\theta_n))(|h_m||g_m|\sin(\theta_m)). \end{aligned} \quad (29)$$

By using the identity $\cos(\alpha + \beta) = \cos(\alpha)\cos(\beta) - \sin(\alpha)\sin(\beta)$, we obtain

$$\begin{aligned}
 X^2 + Y^2 &= \sum_{n=1}^N |h_n|^2 |g_n|^2 \\
 &\quad + \sum_{n=1}^N \sum_{m \neq n=1}^N |h_n| |g_n| |h_m| |g_m| \cos(\theta_n - \theta_m) \\
 &\stackrel{(a)}{\geq} \sum_{n=1}^N |h_n|^2 |g_n|^2 + \varepsilon_{\min} \sum_{n=1}^N \sum_{m \neq n=1}^N |h_n| |g_n| |h_m| |g_m| \\
 &\stackrel{(b)}{\geq} \sum_{n=1}^N |h_n|^2 |g_n|^2, \tag{30}
 \end{aligned}$$

and

$$\begin{aligned}
 X^2 + Y^2 &= \sum_{n=1}^N |h_n|^2 |g_n|^2 \\
 &\quad + \sum_{n=1}^N \sum_{m \neq n=1}^N |h_n| |g_n| |h_m| |g_m| \cos(\theta_n - \theta_m) \\
 &\stackrel{(c)}{\leq} \sum_{n=1}^N |h_n|^2 |g_n|^2 + \sum_{n=1}^N \sum_{m \neq n=1}^N |h_n| |g_n| |h_m| |g_m| \\
 &= \left(\sum_{n=1}^N |h_n| |g_n| \right)^2, \tag{31}
 \end{aligned}$$

where (a) and (b) follow under the assumption $\varepsilon_{\min} \geq 0$, and (c) follows because $\cos(\theta_n - \theta_m) \leq 1$ for any phase errors. This concludes the proof. ■

Proposition 9: If $\varepsilon_{\min} = \min_{n \neq m \in [1, N]} \{\cos(\theta_n - \theta_m)\} \geq 0$, RIS-assisted transmission achieves the full diversity order in the presence of phase noise.

Proof: It follows from Proposition 8, by noting the following: (i) the upper bound in (31) coincides with the SNR in the absence of phase errors, which is shown to achieve the full diversity order in Section III, and (ii) the lower bound in (30) is the SNR of an equivalent maximal-ratio combining system whose links have an SNR equal to $|h_n|^2 |g_n|^2$. From [36], the diversity order of the lower bounds in (30) is the same as the diversity order of the upper bound in (31), since the latter bound corresponds to the SNR (scaled by a fixed constant) of an equivalent equal-gain combining system. This concludes the proof. ■

Remark 4: The upper bound in (31) can be applied only if $\varepsilon_{\min} = \min_{n \neq m \in [1, N]} \{\cos(\theta_n - \theta_m)\} \geq 0$. This implies that Proposition 9 yields a sufficient condition for achieving the full diversity order. If $\varepsilon_{\min} = \min_{n \neq m \in [1, N]} \{\cos(\theta_n - \theta_m)\} < 0$, in other words, a diversity loss may occur.

Based on Proposition 8 and Proposition 9, the following remarks can be made:

- The condition $\varepsilon_{\min} = \min_{n \neq m \in [1, N]} \{\cos(\theta_n - \theta_m)\} \geq 0$ implies that the absolute difference between pairs of

phase errors is always less than $\pi/2$. This yields important guidelines to make the design of RISs robust to the phase noise.

- Assume that the phase noise is determined by the number L of quantization bits used. Then, by definition, we have $\cos(2\pi/2^L) \leq \cos(\theta_n - \theta_m) \leq 1$. This yields $\varepsilon_{\min} = \cos(\pi) = -1$ for $L = 1$, $\varepsilon_{\min} = \cos(\pi/2) = 0$ for $L = 2$, and $\varepsilon_{\min} > 0$ for $L > 2$. Therefore, the full diversity order can be ensured if at least two quantization bits are used. This result is in agreement with [19], but generalizes it to arbitrary fading distributions and phase noise distributions.
- The potential loss of diversity for $\varepsilon_{\min} = \min_{n \neq m \in [1, N]} \{\cos(\theta_n - \theta_m)\} < 0$ can be understood by considering the case study for $N = 2$ and $L = 1$ in Proposition 8. In this case, we obtain $X^2 + Y^2|_{\text{worst case}} = (|h_1| |g_1| - |h_2| |g_2|)^2$. The negative sign in the latter equation is responsible for the potential loss of diversity order for $\varepsilon_{\min} < 0$.

In conclusion, with the aid of the sufficient condition identified in Proposition 9, an RIS can be appropriately optimized in order to guarantee that the full diversity order is achieved. To the best of our knowledge, this result for arbitrary fading and phase noise distributions was never reported in the literature. A similar approach could be applied to the analysis of hardware impairments different from the phase noise.

V. NUMERICAL RESULTS

In this section, we report some numerical results in order to substantiate the obtained analytical expressions of the outage probability and the analysis of the diversity order and coding gain with the aid of Monte Carlo simulations. Unless otherwise stated, the SNR threshold is set to $\gamma_{th} = 0$ dB. It is worth mentioning that the numerical results consider relatively small values of N in order to better highlight the impact of the diversity order, which is the main focus of the present paper, similar to [19].

Figure 1 shows the outage probability of an RIS-assisted system in the absence of phase noise as a function of the average SNR (i.e., ρ), for several values of N and under Nakagami- m fading for $m_i^g > m_i^h$, $i = 1, \dots, N$, with $\min_{i=1, \dots, N} \{m_i^h\} = 0.5$. We observe that the exact expression of the outage probability in (4) and its corresponding high-SNR approximation in (14) are in close agreement with Monte Carlo simulations. In particular, Fig. 1 confirms that correctness of the diversity analysis in Section III-A. As expected, the outage probability decreases significantly as the number N of reconfigurable elements of the RIS increases.

Figure 2 shows the outage probability vs. the average SNR ρ over α - μ fading in both i.i.d and i.n.i.d. scenarios. The conclusions are similar to those in Fig. 1. We observe, in particular, that the outage probability over i.n.i.d. α - μ fading decreases at a rate of $\rho^{-\sum_{i=1}^N \frac{\min\{\alpha_i^h \mu_i^h, \alpha_i^g \mu_i^g\}}{2}}$, in agreement with (12) and more precisely with (14) and (16), under

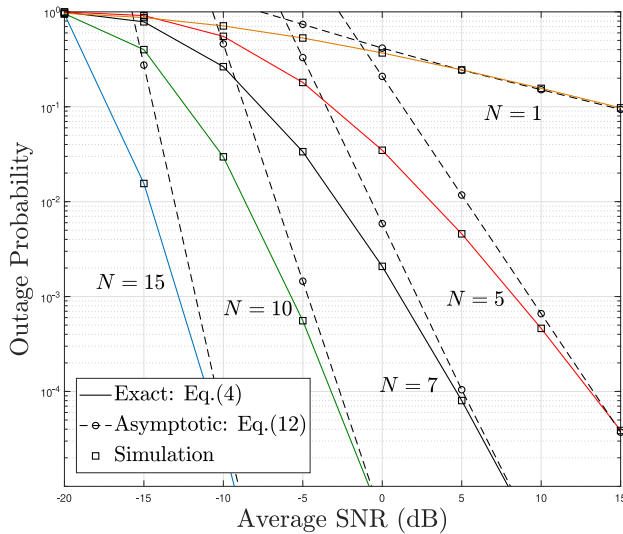


FIGURE 1. Outage probability vs. the average SNR in Nakagami- m fading.

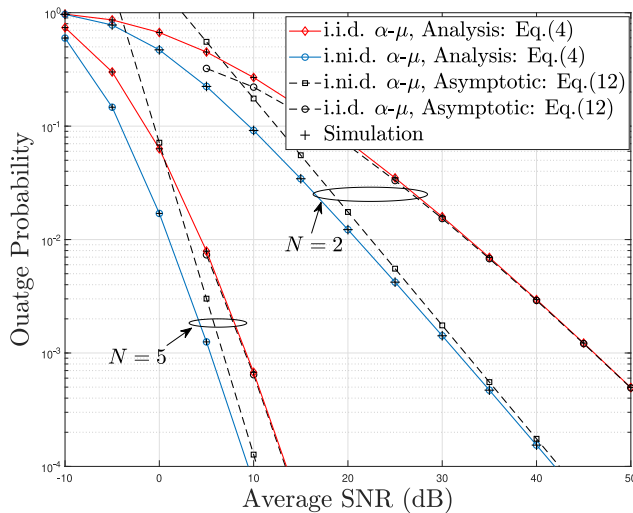


FIGURE 2. Outage probability vs. the average SNR in α - μ fading.

the assumptions of Scenario 1. Over i.i.d. fading, in addition, the figure confirms that the outage probability scales with $\ln(\rho)/\rho$, as predicted by (16), under the assumptions of Scenario 2, and unveiled in [16] and [19] over i.i.d. Rayleigh fading channels.

Figure 3 illustrates the outage probability of an RIS-aided system in the presence of phase noise over Nakagami- m fading. The phase noise is modeled by assuming that the phases are quantized by using $L = 1$ and $L = 2$ quantization bits. The numerical results obtained with Monte Carlo simulations are in agreement with the analytical findings in Section IV. The figure confirms, in particular, that the CLT does not yield, in general, an accurate estimate of the diversity order. In addition, we observe, that a two-bit quantization ($L = 2$) for the phase shifts yields, in the considered case study, sufficiently good performance in terms

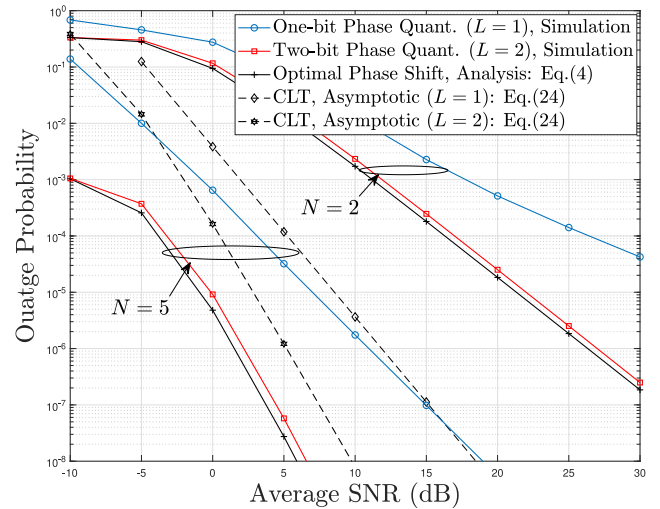


FIGURE 3. Outage probability vs. the average SNR, for different values of L and N (Nakagami- m fading with $m = 1.5$).

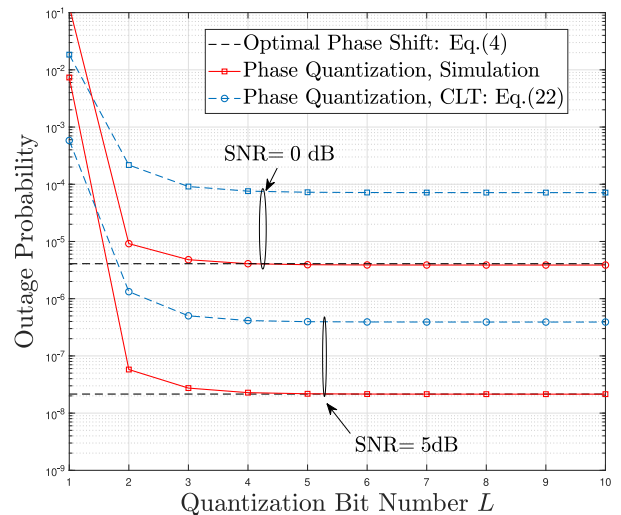


FIGURE 4. Outage probability vs. L over Nakagami- m fading ($m = 1.5$) for different values of the average SNR and $N = 4$.

of outage probability. In particular, the full diversity order can be achieved, as stated in Proposition 9.

Figure 4 shows the outage probability as a function of the number of quantization bits for the phase shifts of the RIS. Figure 4 further corroborates the performance trends illustrated in Fig. 3. In particular, we observe that $L = 3$ provides an outage probability that is close to the setup in the absence of phase noise. Furthermore, Fig. 4 confirms that the CLT does not provide reliable estimates of the outage probability in the considered setup.

VI. CONCLUSION

In this paper, we have introduced a comprehensive analytical framework for analyzing the outage probability and diversity order of RIS-assisted communication systems over generalized fading channels and in the presence of phase noise. The proposed approach leverages the analytical formalism

of the Fox's H functions. We have substantiated, over generalized fading channels, that the central limit theorem is not, in general, a suitable approach for analyzing the diversity order of RIS-aided systems. Therefore, we have introduced a new analytical approach for computing the diversity order in the absence of phase noise, and we have identified sufficient conditions for ensuring that the full diversity order is achieved in the presence of phase noise. In particular, we have proved that RIS-assisted communications achieve the full diversity order provided that the absolute difference between pairs of phase errors is less than $\pi/2$. The obtained findings are shown to be in agreement and to generalize previous results available in the literature.

APPENDIX A

By defining $\mathcal{S} = \sum_{i=1}^N |h_i||g_i|$, we have [44]

$$\Pi(\rho, N) = \frac{1}{2\pi j} \int_{\mathcal{C}} s^{-1} \Psi_{\mathcal{S}}(s) e^{s\sqrt{\rho}} ds, \quad (32)$$

where $\Psi_{\mathcal{S}}(s) = \prod_{i=1}^N \mathcal{L}(f_{|h_i||g_i|})(s)$, and $\mathcal{L}(\cdot)$ stands for the Laplace transform. Next, applying [45, Th. (4.1)] for the pdf of the product of two Fox's H distributions $f_{|h_i||g_i|}$, then evaluating the Laplace transform of $f_{|h_i||g_i|}$, with the help of [43, eq. (2.20)], yield $\Psi_{\mathcal{S}}$ as shown in (33) at the bottom of this page. By plugging (33) into (32), the outage probability can be written as in (34) shown at the bottom of this page. The desired result follows by recalling that $\frac{1}{2\pi j} \int_{\mathcal{C}} s^{-a} e^{sz} ds = \frac{z^{a-1}}{\Gamma(a)}$ and by capitalizing on the multiple Mellin–Barnes type contour integral of the multivariate Fox's H function [43, Def. A.1] with the aid of some algebraic manipulations.

APPENDIX B

For sufficiently large N , the distribution of $H_b = \frac{1}{N} H$ tends to a non-circularly symmetric complex Gaussian RV where $X = \text{Re}\{H\} = \frac{1}{N} \sum_{i=1}^N |h_i||g_i| \cos(\theta_i)$ and

$Y = \text{Im}\{H\} = \frac{1}{N} \sum_{i=1}^N |h_i||g_i| \sin(\theta_i)$ are approximately Gaussian due to the CLT. In particular, $X \sim \mathcal{N}(v, \sigma_X^2)$ and $Y \sim \mathcal{N}(0, \sigma_Y^2)$, where, by using the second-order statistic computation method in [54], we obtain $v = \mathcal{K}_1 \Lambda_1 \Lambda_2$, $\sigma_X^2 = \frac{1}{2N} (1 + \mathcal{K}_2 - 2\mathcal{K}_1^2 \Lambda_1^2 \Lambda_2^2)$, and $\sigma_Y^2 = \frac{1}{2N} (1 - \mathcal{K}_2)$, where

$$\Lambda_1 = \mathbb{E}\{|h_i|\} \text{ and } \Lambda_2 = \mathbb{E}\{|g_i|\}, \quad (35)$$

which, using (2), is computed using the Mellin transform of the Fox's H function [43, eq. (2.8)].⁴

Moreover, since the considered phase errors distributions are symmetric around their mean value that is equal to zero, we obtain $\mathbb{E}\{XY\} = 0$. Hence, X and Y are uncorrelated RVs, and, hence, as normal RVs, independent. Accordingly, $|H_b|^2$ is the sum of a scaled non-central chi-squared RV X^2 and a gamma variable Y^2 , which are mutually independent. Thus, we have

$$\mathcal{L}f_{|H_b|^2}(s) = \mathcal{L}f_{X^2}(s) \mathcal{L}f_{Y^2}(s) = \frac{e^{-\frac{v^2 s}{1+2\sigma_X^2 s}}}{\sqrt{1+2\sigma_X^2 s} \sqrt{1+2\sigma_Y^2 s}}. \quad (36)$$

By applying the same steps as in (34), i.e., by computing the inverse Laplace transform of (36), the distribution of $|H_b|^2$ can be formulated as

$$\begin{aligned} \mathbb{P}(|H_b|^2 < t) &= \mathcal{L}^{-1} \left\{ s^{-1} \mathcal{L}f_{|H_b|^2}(s), t \right\} \stackrel{(a)}{=} \sum_{k=0}^{\infty} \frac{(-1)^k (v^2)^k}{k!} \\ &\quad \mathcal{L}^{-1} \left\{ \frac{s^{k-1}}{(1+2\sigma_X^2 s)^{k+\frac{1}{2}} (1+2\sigma_Y^2 s)^{\frac{1}{2}}}, t \right\}, \end{aligned} \quad (37)$$

where (a) follows by using $e^{-x} = \sum_{k=0}^{\infty} \frac{(-1)^k x^k}{k!}$.

4. For instance, we obtain $\Lambda_i = \frac{\sqrt{\pi}}{2}$, $i = 1, 2$, for Rayleigh fading, $\Lambda_i = \frac{\Gamma(m_i + \frac{1}{2})}{\sqrt{m_i} \Gamma(m_i)}$ for Nakagami- m fading, and $\Lambda_i = \sqrt{\frac{4}{\pi(K_i+1)}} {}_1F_1(-\frac{1}{2}, 1, -K_i)$ in Rician fading, respectively.

$$\begin{aligned} \Psi_{\mathcal{S}}(s) &= \frac{\tau}{(2\pi w)^N} \int_{\mathcal{C}_1} \dots \int_{\mathcal{C}_N} \prod_{i=1}^N \left(\frac{\Gamma(-u_i) \Theta_i(u_i)}{\tilde{c}_i^{u_i}} \right) s^{\sum_{i=1}^N u_i} du_1 du_2 \dots du_N \\ \text{where } w &= \sqrt{-1}, \quad \Theta_j(u_j) = \frac{\prod_{j=1}^{\tilde{m}_j} \Gamma(\xi_j + \Xi_j u_j) \prod_{j=1}^{\tilde{n}_j} \Gamma(1 - \delta_j - \Delta_j u_j)}{\prod_{j=\tilde{n}_j+1}^{\tilde{p}_j} \Gamma(\delta_j + \Delta_j u_j) \prod_{j=\tilde{m}_j+1}^{\tilde{q}_j} \Gamma(1 - \xi_j - \Xi_j u_j)} \\ \text{and } \mathcal{C}_i, i &= 1, \dots, N \text{ represents the contours } [\tau_i - w\infty, \tau_i + w\infty], \tau \in \mathbb{R} \end{aligned} \quad (33)$$

$$\begin{aligned} \frac{1}{2\pi w} \int_{\mathcal{C}} s^{-1} \Psi_{\mathcal{S}}(s) e^{sz} ds &= \frac{\tau}{(2\pi w)^N} \int_{\mathcal{C}_1} \dots \int_{\mathcal{C}_N} \prod_{i=1}^N \left(\frac{\Gamma(-u_i) \Theta_i(u_i)}{\tilde{c}_i^{u_i}} \right) \\ &\quad \times \frac{1}{2\pi w} \int_{\gamma+w\infty}^{\gamma-w\infty} e^{sz} s^{\sum_{i=1}^N u_i - 1} ds du_1 du_2 \dots du_N \\ &= \frac{\tau}{(2\pi w)^N} \int_{\mathcal{C}_1} \dots \int_{\mathcal{C}_N} \prod_{i=1}^N \left(\frac{\Gamma(-u_i) \Theta_i(u_i)}{\tilde{c}_i^{u_i}} \right) \frac{z^{-\sum_{i=1}^N u_i}}{\Gamma(1 - \sum_{i=1}^N u_i)} du_1 du_2 \dots du_N \end{aligned} \quad (34)$$

Substituting $(1+x)^{-a} = \frac{1}{\Gamma(a)} \int_{\mathcal{L}} \Gamma(s)\Gamma(a-s)x^{-s}ds$ in (37), and applying $\frac{1}{2\pi j} \int_{\mathcal{L}} s^{-a}e^{sz}ds = \frac{z^{a-1}}{\Gamma(a)}$, the distribution of $|H_b|^2$ can be formulated as

$$P(|H_b|^2 < t) = \frac{1}{\pi(2\pi w)^2} \int_{C_1} \int_{C_2} \frac{\Gamma(u_1)\Gamma(u_2)}{(2\sigma_X^2)^{u_1}(2\sigma_Y^2)^{u_2}} t^{u_1+u_2} \frac{\Gamma(\frac{1}{2}-u_1)\Gamma(\frac{1}{2}-u_2)}{\Gamma(1+u_1+u_2)} {}_2F_1\left(\frac{1}{2}-u_1, -u_1-u_2, \frac{1}{2}, \frac{v^2}{t}\right) du_1 du_2, \quad (38)$$

where ${}_2F_1(\cdot)$ denotes the Gauss hypergeometric function [52]. Using the representation of the ${}_2F_1(\cdot)$ hypergeometric function in terms of Mellin-Barnes integrals [43], we obtain (39) shown at the bottom of this page.

From (18), the outage probability for large N is obtained as

$$\Pi(\rho, N) = P\left(|H_b|^2 < \frac{\gamma_{th}}{N^2 \rho}\right). \quad (40)$$

However, in the obtained current form, the distribution of $|H_b|^2$ in (39) involves an undermined form in the high-SNR regime. When $t \rightarrow 0$, more precisely, we have

$$\lim_{N \rightarrow \infty} \lim_{t \rightarrow 0} \frac{v^2 t}{\sigma_X^2} = \lim_{N \rightarrow \infty} \lim_{t \rightarrow 0} \frac{v^2 t}{\sigma_Y^2} = 0 \times \infty. \quad (41)$$

To circumvent this, we use the Euler-Gauss limit [52] for $Z \in \{\frac{v^2}{2\sigma_X^2}, \frac{v^2}{2\sigma_Y^2}\}$ as

$$Z^s \underset{N \gg 1}{\approx} \frac{\Gamma(Z-s)}{\Gamma(Z-2s)}, \quad (42)$$

Based on (42), we obtain (43), shown at the bottom of this page. By applying [43, eq. (A.1)] to (43) and using the identity $\Gamma(\frac{1}{2}-u_3) = \frac{\Gamma(-2u_3)2^{2u_3+1}\sqrt{\pi}}{\Gamma(-u_3)}$, we obtain (22) after some manipulations.

If the phase noise has a uniform distribution over $[-\pi, \pi]$, we have ${}_2F_1(\frac{1}{2}-u_2, -u_1-u_2, 0) = 1$ in (38), since $v = 0$.

Substituting $\sigma_X^2 = \sigma_Y^2 = \frac{1}{2N}$, and using the Euler-Gauss limit [52]

$$N^s \underset{N \gg 1}{\approx} \frac{\Gamma(N-s)}{\Gamma(N-2s)}, \quad (44)$$

we obtain

$$P(|H_b|^2 < t) = \frac{1}{\pi(2\pi w)^2} \times \int_{C_1} \int_{C_2} \Gamma(u_1)\Gamma(u_2) \frac{\Gamma(\frac{1}{2}-u_1)\Gamma(\frac{1}{2}-u_2)}{\Gamma(1+u_1+u_2)} \frac{\Gamma(N-u_1)}{\Gamma(N-2u_1)} \frac{\Gamma(N-u_2)}{\Gamma(N-2u_2)} t^{u_1+u_2} du_1 du_2, \quad (45)$$

which leads to (23) with the aid of [43, eq. (A.1)]. This completes the proof.

APPENDIX C

It is worth noting that other performance metrics, including the ergodic capacity, error probability and secrecy rate can be addressed by leveraging the analytical methodology developed in the paper. In particular, recalling (4), the average bit error probability (ABEP) can be expressed as [50]

$$\mathcal{B} = \frac{q^p}{2\Gamma(p)} \int_0^\infty x^{p-1} e^{-qx} \Pi\left(\frac{x}{\rho}, N\right) dx, \quad (46)$$

where p and q are modulation specific parameters. For instance, $(p, q) = (0.5, 1)$ denotes the binary shift keying (BPSK), $(p, q) = (0.5, 0.5)$ for coherent binary frequency shift keying, and $(p, q) = (1, 1)$ for differential BPSK. The ABEP is evaluated by plugging (4) into (46) while resorting to [52, eq. (3.351.3)] and [52, eq. (8.331.1)] to express $\int_0^\infty z^{-\frac{\sum_{i=1}^N u_i}{2} + p - 1} e^{-qz} dz = q^{\frac{\sum_{i=1}^N u_i}{2} - p} \Gamma(p - \frac{\sum_{i=1}^N u_i}{2})$, thereby yielding (47) shown at the top of the next page. Following similar procedures as for (12) and (13), we can obtain the ABEP asymptotic expansions by resorting to the residue theorem [49].

$$P(|H_b|^2 < t) = \frac{1}{\sqrt{\pi}(2\pi w)^3} \times \int_{C_1} \int_{C_2} \int_{C_3} \frac{\Gamma(u_1)\Gamma(u_2)\Gamma(u_3)}{\left(\frac{2\sigma_X^2}{v^2 t}\right)^{u_1} \left(\frac{2\sigma_Y^2}{v^2 t}\right)^{u_2} (-v^2)^{u_1+u_2+u_3}} \frac{\Gamma(\frac{1}{2}-u_1-u_3)\Gamma(-u_1-u_2-u_3)\Gamma(\frac{1}{2}-u_2)}{\Gamma(1+u_1+u_2)\Gamma(\frac{1}{2}-u_3)\Gamma(-u_1-u_2)} t^{u_3} du_1 du_2 du_3 \quad (39)$$

$$P(|H_b|^2 < t) = \frac{1}{\sqrt{\pi}(2\pi w)^3} \times \int_{C_1} \int_{C_2} \int_{C_3} \Gamma(u_1)\Gamma(u_2)\Gamma(u_3) \frac{\Gamma(\frac{1}{2}-u_1-u_3)\Gamma(-u_1-u_2-u_3)\Gamma(\frac{1}{2}-u_2)}{\Gamma(1+u_1+u_2)\Gamma(\frac{1}{2}-u_3)\Gamma(-u_1-u_2)} \frac{\Gamma\left(\frac{v^2}{2\sigma_X^2}-u_1\right)}{\Gamma\left(\frac{v^2}{2\sigma_X^2}-2u_1\right)} \frac{\Gamma\left(\frac{v^2}{2\sigma_Y^2}-u_2\right)}{\Gamma\left(\frac{v^2}{2\sigma_Y^2}-2u_2\right)} \left(\frac{t}{v^2}\right)^{u_1+u_2} \left(\frac{-t}{v^2}\right)^{u_3} du_1 du_2 du_3 \quad (43)$$

$$\mathcal{B} = \frac{\tau}{2\Gamma(p)} \mathbf{H}_{1,1;\tilde{p}_1,\dots,\tilde{p}_N}^{0,1;\tilde{m}_1,\tilde{m}_1,\dots,\tilde{m}_N,\tilde{m}_N} \left[\begin{array}{c} \tilde{c}_1 \sqrt{q\rho} \\ \vdots \\ \tilde{c}_N \sqrt{q\rho} \end{array} \middle| \begin{array}{l} (1-p; 1, \dots, 1) : (1, 1), (\delta_1, \Delta_1)_{\tilde{p}_1}; \dots; (1, 1), (\delta_N, \Delta_N)_{\tilde{p}_N} \\ (0; 1, \dots, 1) : (\xi_1, \Xi_1)_{\tilde{q}_1}; \dots; (\xi_N, \Xi_N)_{\tilde{q}_N} \end{array} \right] \quad (47)$$

REFERENCES

- [1] K. B. Letaief, W. Chen, Y. Shi, J. Zhang, and Y.-J. A. Zhang, "The roadmap to 6G: AI empowered wireless networks," *IEEE Commun. Mag.*, vol. 57, no. 8, pp. 84–90, Aug. 2019.
- [2] M. A. ElMossallamy, H. Zhang, L. Song, K. G. Seddik, Z. Han, and G. Y. Li, "Reconfigurable intelligent surfaces for wireless communications: Principles, challenges, and opportunities," *IEEE Trans. Cogn. Commun. Netw.*, vol. 6, no. 3, pp. 990–1002, Sep. 2020.
- [3] E. Basar, M. Di Renzo, J. de Rosny, M. Debbah, M.-S. Alouini, and R. Zhang, "Wireless communications through reconfigurable intelligent surfaces," *IEEE Access*, vol. 7, pp. 116753–116773, 2019.
- [4] M. Di Renzo *et al.*, "Reconfigurable intelligent surfaces vs. relaying: Differences, similarities, and performance comparison," *IEEE Open J. Commun. Soc.*, vol. 1, pp. 798–807, 2020.
- [5] M. Di Renzo *et al.*, "Smart radio environments empowered by reconfigurable intelligent surfaces: How it works, state of research, and the road ahead," *IEEE J. Sel. Areas Commun.*, vol. 38, no. 11, pp. 2450–2525, Nov. 2020.
- [6] Q. Wu and R. Zhang, "Towards smart and reconfigurable environment: Intelligent reflecting surface aided wireless network," *IEEE Commun. Mag.*, vol. 58, no. 1, pp. 106–112, Jan. 2020.
- [7] Q. Wu and R. Zhang, "Intelligent reflecting surface enhanced wireless network via joint active and passive beamforming," *IEEE Trans. Wireless Commun.*, vol. 18, no. 11, pp. 5394–5409, Nov. 2019.
- [8] M. A. Saeidi, M. J. Emadi, H. Masoumi, M. R. Mili, D. W. K. Ng, and I. Krikidis, "Weighted sum-rate maximization for multi-IRS-assisted full-duplex systems with hardware impairments," *IEEE Trans. Cogn. Commun. Netw.*, vol. 7, no. 2, pp. 466–481, Jun. 2021.
- [9] B. Di, H. Zhang, L. Li, L. Song, Y. Li, and Z. Han, "Practical hybrid beamforming with finite-resolution phase shifters for reconfigurable intelligent surface based multi-user communications," *IEEE Trans. Veh. Technol.*, vol. 69, no. 4, pp. 4565–4570, Apr. 2020.
- [10] Y. Wang, H. Lu, D. Zhao, Y. Deng, and A. Nallanathan, "Intelligent reflecting surface-assisted mmWave communication with lens antenna array," *IEEE Trans. Cogn. Commun. Netw.*, vol. 8, no. 1, pp. 202–215, Mar. 2022.
- [11] L. Yang, F. Meng, J. Zhang, M. O. Hasna, and M. Di Renzo, "On the performance of RIS-assisted dual-hop UAV communication systems," *IEEE Trans. Veh. Technol.*, vol. 69, no. 9, pp. 10385–10390, Sep. 2020.
- [12] I. Trigui, W. Ajib, and W.-P. Zhu, "Secrecy outage probability and average rate of RIS-aided communications using quantized phases," *IEEE Commun. Lett.*, vol. 25, no. 6, pp. 1820–1824, Jun. 2021.
- [13] S. Zargari, S. Farahmand, B. Abolhassani, and C. Tellambura, "Robust active and passive beamformer design for IRS-aided downlink MISO PS-SWIPT with a nonlinear energy harvesting model," *IEEE Trans. Green Commun. Netw.*, vol. 5, no. 4, pp. 2027–2041, Dec. 2021.
- [14] Z. Ding, R. Schober, and H. V. Poor, "On the impact of phase shifting designs on IRS-NOMA," *IEEE Wireless Commun. Lett.*, vol. 9, no. 10, pp. 1596–1600, Oct. 2020.
- [15] A.-A. A. Boulogeorgos and A. Alexiou, "Performance analysis of reconfigurable intelligent surface-assisted wireless systems and comparison with relaying," *IEEE Access*, vol. 8, pp. 94463–94483, 2020.
- [16] S. Atapattu, R. Fan, P. Dharmawansa, G. Wang, J. Evans, and T. A. Tsiftsis, "Reconfigurable intelligent surface assisted two-way communications: Performance analysis and optimization," *IEEE Trans. Commun.*, vol. 68, no. 10, pp. 6552–6567, Oct. 2020.
- [17] D. Kudathanthirige, D. Gunasinghe, and G. Amarasinghe, "Performance analysis of intelligent reflective surfaces for wireless communication," in *Proc. IEEE Int. Commun. Conf.*, 2020, pp. 1–6.
- [18] M.-A. Badiu and J. P. Coon, "Communication through a large reflecting surface with phase errors," *IEEE Wireless Commun. Lett.*, vol. 9, no. 2, pp. 184–188, Feb. 2020.
- [19] P. Xu, G. Chen, Z. Yang, and M. Di Renzo, "Reconfigurable intelligent surfaces-assisted communications with discrete phase shifts: How many quantization levels are required to achieve full diversity?" *IEEE Wireless Commun. Lett.*, vol. 10, no. 2, pp. 358–362, Feb. 2021.
- [20] X. Qian, M. Di Renzo, J. Liu, A. Kammoun, and M.-S. Alouini, "Beamforming through reconfigurable intelligent surfaces in single-user MIMO systems: SNR distribution and scaling laws in the presence of channel fading and phase noise," *IEEE Wireless Commun. Lett.*, vol. 10, no. 1, pp. 77–81, Jan. 2021.
- [21] L. Yang, Y. Yang, D. B. da Costa, and I. Trigui, "Outage probability and capacity scaling law of multiple RIS-aided networks," *IEEE Wireless Commun. Lett.*, vol. 10, no. 2, pp. 256–260, Feb. 2021.
- [22] S. Li, L. Yang, D. B. da Costa, M. Di Renzo, and M.-S. Alouini, "On the performance of RIS-assisted dual-hop mixed RF-UWOC systems," *IEEE Trans. Cogn. Commun. Netw.*, vol. 7, no. 2, pp. 340–353, Jun. 2021.
- [23] T. Wang, G. Chen, J. P. Coon, and M.-A. Badiu, "Chernoff bound and saddlepoint approximation for outage probability in IRS-assisted wireless systems," in *Proc. IEEE Globecom Workshops*, Dec. 2021, pp. 1–5.
- [24] T. Wang, G. Chen, J. P. Coon, and M.-A. Badiu, "Study of intelligent reflective surface assisted communications with one-bit phase adjustments," in *Proc. IEEE Globecom Workshops*, Dec. 2020, pp. 1–6.
- [25] Q. Tao, J. Wang, and C. Zhong, "Performance analysis of intelligent reflecting surface aided communication systems," *IEEE Commun. Lett.*, vol. 24, no. 11, pp. 2464–2468, Nov. 2020.
- [26] L. Yang, F. Meng, Q. Wu, D. B. da Costa, and M.-S. Alouini, "Accurate closed-form approximations to channel distributions of RIS-aided wireless systems," *IEEE Wireless Commun. Lett.*, vol. 9, no. 11, pp. 1985–1989, Nov. 2020.
- [27] J. Lyu and R. Zhang, "Spatial throughput characterization for intelligent reflecting surface aided multiuser system," *IEEE Wireless Commun. Lett.*, vol. 6, no. 9, pp. 834–838, Jun. 2020.
- [28] M. Jung, W. Saad, Y. R. Jang, G. Kong, and S. Choi, "Performance analysis of large intelligent surfaces (LISs): Asymptotic data rate and channel hardening effects," *IEEE Trans. Wireless Commun.*, vol. 19, no. 3, pp. 2052–2065, Mar. 2020.
- [29] Q.-U.-A. Nadeem, A. Kammoun, A. Chaaban, M. Debbah, and M.-S. Alouini, "Asymptotic max–min SINR analysis of reconfigurable intelligent surface assisted MISO systems," *IEEE Trans. Wireless Commun.*, vol. 19, no. 12, pp. 7748–7764, Dec. 2020.
- [30] Z. Zhang, Y. Cui, F. Yang, and L. Ding, "Analysis and optimization of outage probability in multi-intelligent reflecting surface-assisted systems," 2019, *arXiv:1909.02193*.
- [31] I. Trigui, E. K. Agbogla, M. Benjillali, W. Ajib, and W.-P. Zhu, "Bit error rate analysis for reconfigurable intelligent surfaces with phase errors," *IEEE Commun. Lett.*, vol. 25, no. 7, pp. 2176–2180, Jul. 2021.
- [32] R. C. Ferreira, M. S. P. Facina, F. A. P. De Figueiredo, G. Fraidenraich, and E. R. De Lima, "Bit error probability for large intelligent surfaces under double-Nakagami fading channels," *IEEE Open J. Commun. Soc.*, vol. 1, pp. 750–759, 2020.
- [33] D. Selimis, K. P. Peppas, G. C. Alexandropoulos, and F. I. Lazarakis, "On the performance analysis of RIS-empowered communications over Nakagami- m fading," *IEEE Commun. Lett.*, vol. 25, no. 7, pp. 2191–2195, Jul. 2021.
- [34] H. Ibrahim, H. Tabassum, and U. T. Nguyen, "Exact coverage analysis of intelligent reflecting surfaces with Nakagami- m channels," *IEEE Trans. Veh. Technol.*, vol. 70, no. 1, pp. 1072–1076, Jan. 2021.
- [35] J. Gil-Pelaez, "Note on the inversion theorem," *Biometrika*, vol. 38, nos. 3–4, pp. 481–482, 1951.
- [36] Z. Wang and G. B. Giannakis, "A simple and general parameterization quantifying performance in fading channels," *IEEE Trans. Commun.*, vol. 51, no. 8, pp. 1389–1398, Aug. 2003.

- [37] A.-A. A. Boulogeorgos and A. Alexiou, "How much do hardware imperfections affect the performance of reconfigurable intelligent surface-assisted systems?" *IEEE Open J. Commun. Soc.*, vol. 1, pp. 1185–1195, 2020.
- [38] F. H. Danufane, M. Di Renzo, J. de Rosny, and S. Tretyakov, "On the path-loss of reconfigurable intelligent surfaces: An approach based on Green's theorem applied to vector fields," *IEEE Trans. Commun.*, vol. 69, no. 8, pp. 5573–5592, Aug. 2021.
- [39] W. Tang *et al.*, "Wireless communications with reconfigurable intelligent surface: Path loss modeling and experimental measurement," *IEEE Trans. Wireless Commun.*, vol. 20, no. 1, pp. 421–439, Jan. 2021.
- [40] S. Abeywickrama, R. Zhang, Q. Wu, and C. Yuen, "Intelligent reflecting surface: Practical phase shift model and beamforming optimization," *IEEE Trans. Commun.*, vol. 68, no. 3, pp. 5849–5863, Sep. 2020.
- [41] A. Zappone, M. Di Renzo, F. Shams, X. Qian, and M. Debbah, "Overhead-aware design of reconfigurable intelligent surfaces in smart radio environments," *IEEE Trans. Wireless Commun.*, vol. 20, no. 1, pp. 126–141, Jan. 2021.
- [42] F. Yilmaz and M.-S. Alouini, "A novel unified expression for the capacity and bit error probability of wireless communication systems over generalized fading channels," *IEEE Trans. Commun.*, vol. 60, no. 7, pp. 1862–1876, Jul. 2012.
- [43] A. M. Mathai, R. K. Saxena, and H. J. Haubold, *The H-Function: Theory and Applications*. New York, NY, USA: Springer, 2009.
- [44] I. Trigui and S. Affes, "Unified analysis and optimization of D2D communications in cellular Networks over fading channels," *IEEE Trans. Commun.*, vol. 67, no. 1, pp. 724–736, Jan. 2019.
- [45] I. Cook, Jr., "The H-function and probability density functions of certain algebraic combinations of independent random variables with H-function probability distribution," DTIC, Fort Belvoir, VA, USA, Rep. 81–47D, 1981.
- [46] H. R. Alhennawi, M. M. H. El Ayadi, M. H. Ismail, and H.-A. M. Mourad, "Closed-form exact and asymptotic expressions for the symbol error rate and capacity of the H-function fading channel," *IEEE Trans. Veh. Technol.*, vol. 65, no. 4, pp. 1957–1974, Apr. 2016.
- [47] H. Chergui, M. Benjillali, and M.-S. Alouini, "Rician K-factor-based analysis of XLOS service probability in 5G outdoor ultra-dense networks," *IEEE Wireless Commun. Lett.*, vol. 8, no. 2, pp. 428–431, Apr. 2019.
- [48] M. K. Simon and M.-S. Alouini, *Digital Communication Over Fading Channels*. Hoboken, NJ, USA: Wiley, 2005.
- [49] A. Kilbas and M. Saigo, *H-Transforms: Theory and Applications*. Boca Raton, FL, USA: CRC Press, 2004.
- [50] C. M. Lo and W. H. Lam, "Error probability of binary phase shift keying in Nakagami-*m* fading channel with phase noise," *Electron. Lett.*, vol. 26, no. 21, pp. 1773–1774, Oct. 2000.
- [51] R. K. Saxena, "On the H-function of *n* variables," *Kyungpook Math. J.*, vol. 17, no. 2, pp. 221–226, 1977.
- [52] I. Gradshteyn and I. Ryzhik, *Table of Integrals, Series, and Products*. San Diego, CA, USA: Academic, 1994.
- [53] W. Rudin, *Real and Complex Analysis*, 3rd ed. New York, NY, USA: McGraw-Hill, 1987.
- [54] B. Picinbono, "Second-order complex random vectors and normal distributions," *IEEE Trans. Signal Process.*, vol. 44, no. 10, pp. 2637–2640, Oct. 1996.

IMÈNE TRIGUI (Member, IEEE) received the M.Sc. and Ph.D. degrees (Highest Hons.) from the National Institute of Scientific Research (INRS-EMT), University of Quebec, Montreal, QC, Canada. From 2016 to 2018, she was a Postdoctoral Research Fellow with the Department of Electrical Engineering, Toronto University, Toronto, ON, Canada. From 2018 to 2019, she was a Research Scientist with INRS-EMT, and since 2020 a RESMIQ Postdoctoral Fellow with the University of Quebec at Montreal. In recognition of her academic, research, and scholarly achievements, she was the recipient of several major awards, including the Natural Sciences and Engineering Research Council of Canada (NSERC) Postdoctoral Fellowship (2016–2018) and the top-tier Alexander-Graham-Bell Canada Graduate Scholarship from the National Sciences and Engineering Research Council (2012–2014). She also received a Best Paper Award at IEEE VTC'2010-Fall. She serves regularly as a reviewer for many top international journals and conferences in her field.

WESSAM AJIB (Senior Member, IEEE) received an Engineer Diploma degree in physical instruments from INPG, Grenoble, France, in 1996, and the master's and Ph.D. degrees in computer networks from École Nationale Supérieure des Télécommunications, Paris, in 1997 and 2000, respectively. He had been an Architect and a Radio Network Designer with Nortel Networks, Ottawa, ON, Canada, from October 2000 to June 2004. He had conducted many outbreaking projects on the third generation of wireless cellular networks. He followed a Postdoctoral Fellowship with École Polytechnique de Montréal, Montreal, QC, Canada, from 2004 to 2005. Since June 2005, he has been with the Department of Computer Sciences, Université du Québec at Montreal, Montreal, where he is currently a Full Professor. He has authored or coauthored many journal papers and conferences papers in these areas. His research interests include wireless communications and networks, multiple access design, and traffic scheduling, machine learning algorithms for wireless networks, resource allocation in 5G and 6G.

WEI-PING ZHU (Senior Member, IEEE) received the B.E. and M.E. degrees in electrical engineering from the Nanjing University of Posts and Telecommunications in 1982 and 1985, respectively, and the Ph.D. degree in electrical engineering from Southeast University, Nanjing, China, in 1991. He was a Postdoctoral Fellow from 1991 to 1992 and a Research Associate from 1996 to 1998 with the Department of Electrical and Computer Engineering, Concordia University, Montreal, Canada. From 1993 to 1996, he was an Associate Professor with the Department of Information Engineering, Nanjing University of Posts and Telecommunications. From 1998 to 2001, he worked with Hi-Tech Companies, Ottawa, Canada, including Nortel Networks and SR Telecom Inc. Since July 2001, he has been with Concordia's Electrical and Computer Engineering Department as a Full-Time Faculty Member, where he is presently a Full Professor. His research interests include digital signal processing and machine learning, speech and statistical signal processing, and signal processing for wireless communication with a particular focus on MIMO systems and cooperative communication. He was the Secretary of Digital Signal Processing Technical Committee (DSPTC) of the IEEE Circuits and System Society from June 2012 to May 2014, and the Chair of the DSPTC from June 2014 to May 2016. He served as an Associate Editor for the IEEE TRANSACTIONS ON CIRCUITS AND SYSTEMS—PART I: FUNDAMENTAL THEORY AND APPLICATIONS from 2001 to 2003, *Circuits, Systems and Signal Processing* from 2006 to 2009, IEEE TRANSACTIONS ON CIRCUITS AND SYSTEMS—PART II: TRANSACTIONS BRIEFS from 2011 to 2015, *Journal of The Franklin Institute* from 2015 to 2019. He was also a Guest Editor for the IEEE JOURNAL ON SELECTED AREAS IN COMMUNICATIONS for the special issues of: Broadband Wireless Communications for High Speed Vehicles, and *Virtual MIMO* from 2011 to 2013. Since January 2020, he has been serving as a Subject Editor for *Journal of The Franklin Institute*.

MARCO DI RENZO (Fellow, IEEE) received the Laurea (*cum laude*) and Ph.D. degrees in electrical engineering from the University of L'Aquila, Italy, in 2003 and 2007, respectively, and the Habilitation à Diriger des Recherches (Doctor of Science) degree from University Paris-Sud (now Paris-Saclay University), France, in 2013. Since 2010, he has been with the French National Center for Scientific Research (CNRS), where he is a CNRS Research Director (Professor) with the Laboratory of Signals and Systems (L2S) of Paris-Saclay University—CNRS and CentraleSupélec, Paris, France. In Paris-Saclay University, he serves as the Coordinator of the Communications and Networks Research Area of the Laboratory of Excellence DigiCosme and as a Member of the Admission and Evaluation Committee of the Ph.D. School on Information and Communication Technologies. He is the Editor-in-Chief of IEEE COMMUNICATIONS LETTERS and a Distinguished Speaker of the IEEE VEHICULAR TECHNOLOGY SOCIETY. From 2017 to 2020, he was a Distinguished Lecturer of the IEEE VEHICULAR TECHNOLOGY SOCIETY and IEEE COMMUNICATIONS SOCIETY. He has received several research distinctions, which include the SEE-IEEE Alain Glavieux Award, the IEEE Jack Neubauer Memorial Best Systems Paper Award, the Royal Academy of Engineering Distinguished Visiting Fellowship, the Nokia Foundation Visiting Professorship, the Fulbright Fellowship, and the 2021 EURASIP Journal on Wireless Communications and Networking Best Paper Award. He is a Fellow of the U.K. Institution of Engineering and Technology and the Asia-Pacific Artificial Intelligence Association, an Ordinary Member of the European Academy of Sciences and Arts and the Academia Europaea. He is also a Highly Cited Researcher.